

MSRC REFERENCE ROOM

MARINE SCIENCES RESEARCH CENTER
STATE UNIVERSITY OF NEW YORK
STONY BROOK, NEW YORK 11794

FINAL REPORT

A STUDY OF THE EFFECTS OF INLET DIMENSIONS
ON SALINITY DISTRIBUTION IN GREAT SOUTH BAY

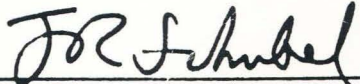
Donald W. Pritchard and Eugenio Gomez-Reyes
June 1986

Prepared For The
County of Suffolk
Department of Planning
H. Lee Dennison Building
Veterans Memorial Highway
Hauppauge, New York

Special Report 70

Reference No. 86-7

Approved for Distribution


J. R. Schubel, Director

FINAL REPORT
A Study of the Effects of Inlet Dimensions
On The Salinity Distribution of Great South Bay

INTRODUCTION

The hard clam industry in Great South Bay (Fig. 1) has suffered a marked decline over the last two decades (McHugh, 1983). No consensus as to the cause of this decline exists among clambers, public officials, resource managers and marine scientists, even though these groups include many who have had long experience in the Bays along the southern shore of Long Island. However, a number of individuals who are now or had in the past been engaged in the harvest of clams have presented the following scenario connecting the decline in clam population in Great South Bay to changes in geometry of the Fire Island Inlet, and specifically, to changes resulting from dredging:

- a) The direct cause of the decline in clam production is an increase in the number of predators in the Bay.
- b) The increase in the number of clam predators results from an increase in salinity in the Bay.
- c) The increase in salinity in the Bay results from dredging in Fire Island Inlet.

Each of the steps in the above scenario has a factual basis: i.e., predation, particularly of juvenile clams, is known to be a limiting factor on clam production (Mackenzie, 1977): certain major species of predators of hard clams are known to be favored by salinity values falling in the upper half of the range of salinities most favorable for growth of hard clams (Walka, 1983): and there is reasonable evidence that an increase in the area of cross sections within Fire Island Inlet, particularly within a critical reach designated as the 'throat' of the inlet, results in an increase in the rate of exchange of Bay water with sea water, and consequently an increase in salinity of the Bay.

The hard clam, Mercenaria mercenaria, grows best in waters having a salt concentration in the range from 24 ‰ to 28 ‰ (U.S. Environmental Protection Agency, 1982). Several species of clam predators do not grow well if the salt concentration is below 27 ‰ and the population density of these predators increase rapidly for salinities above this value (Walka, 1983). Most of Great South Bay has salt concentrations in the range 25 ‰ to 30 ‰ over much of the year (Suffolk County Department of Environmental Control, 1978), and the spatial distribution is such that small changes in the bay-wide mean salinity can result in significant changes in the area of the Bay having salt concentrations greater than 27 ‰.

One of the dredging projects which has been considered by several baymen as contributing to an increase in salinity in Great South Bay involved the removal of a shoal area, called Yellow Bar, located about 1 mile East of the Robert Moses Causeway (Fig. 2). About 1.7 million cubic yards were dredged from this bar during the period April-August, 1970, by the Long Island Park Commission, State of New York, in order to provide fill for the construction of a new parking area at Robert Moses State Park, Fire Island.

The purpose of this study is to test the hypothesis that changes in the dimensions of Fire Island Inlet, such as a large dredging project in the throat region of the Inlet, can lead to changes in the salinity distribution over the Bay. Prior to the removal of Yellow Bar, the cross section at its location was the most restricted along the length of the Inlet. We have used the case of the dredging of Yellow bar as an illustrative example of the hypothesis to be tested. The basic strategy used here was to exercise an hydrodynamic and a salinity model with and without Yellow Bar, keeping all other system parameters fixed, thus isolating the effect of this bar.

A discussion of the theory and practice of numerical simulation of the hydrodynamics and kinematics of water motion and of property distribution in a waterway such as Great South Bay is given in the MA Degree Thesis of Eugenio Gomez-Reyes, entitled "Modification of a Hydrodynamic and a Salinity Finite Element Numerical Model For Application in Bar-Built Estuarine Systems". This Thesis is included in a separately bound Appendix to this report. It contains a detailed description of the particular hydrodynamic and salinity

models used in this study, and of the modifications made to these models to make them applicable to Great South Bay. Also included in the Appendix are detailed explanations of the methods used to obtain the boundary inputs required to drive the models; that is, the fresh water inflow along the northern shoreline of the Bay, and the tidal variation in the water surface elevation at the three open boundaries to Great South Bay. Since many of the readers of this report will be more interested in the results of this study than in the details of how these results were obtained, only summary discussions of the above subjects will be presented in the body of this report. Readers interested in the theory and in the details of the application of the numerical models for the purpose of this study can obtain a copy of the Appendix by contacting Mr. Dewitt Davies, Department of Planning, County of Suffolk, H. Lee Dennison Building, Hauppauge, N.Y..

THE MODELS -- A BRIEF DESCRIPTION

Since previous studies of Great South Bay have shown this waterway to have little or no vertical variation in salinity, temperature, and hence in density, it was concluded that a vertically averaged model would suffice for the purposes of this study. The problem to be treated involves changes in the spatial distribution of salinity due to changes in the geometry of the Inlet, the model must be capable of simulating the two-dimensional geometry of the Bay and Inlet in the horizontal plane. For this type of problem, where a close simulation of the land-water boundaries is necessary, a finite element model is preferable to a finite difference model, since in the latter case the grid is composed of rectangular elements, requiring a stair case type matching of the land boundaries, while in the finite element method triangular elements of varying dimensions are used for the computational grid. Thus, the size of the elements and their orientation are very flexible in a finite element grid. A small element size can be designed along the boundaries of the water body and in regions of particular interest, while in the interior of the system, the element size can be increased.

An important phenomena which must be simulated in any model to be used to attack the problem under consideration here is the tidal rise and fall of the water surface and the resulting tidal current distribution. The tide and the tidal currents are time varying parameters, and hence the model must simulate

this time variation. The model of choice is therefore a transient state vertical averaged two-dimensional finite element model.

Actually, the problem at hand requires the use of two models. One, the hydrodynamic model, involves the numerical solution of the equations of motion, which express Newton's 2nd Law for fluid motion: that is, the rate of change of momentum of a parcel of fluid is set equal to the sum of the forces acting on the parcel. The solution of this hydrodynamic model provide as output the temporal and spatial distribution of the water surface elevation and of the water velocity. These parameters are then used as input to a kinematic model for the calculation of the distribution of salinity. This salinity model involves the solution of the equation for salt continuity, which states that the rate of change of salt concentration is equal to the sum of advective processes and diffusive processes. The advective processes depend on the velocity field input from the output of the hydrodynamic model, while the diffusive terms depend on the coefficient of eddy diffusion. This latter coefficient is obtained as part of the model adjustment and verification process.

A two-dimensional vertically integrated finite element hydrodynamic model developed by Wang and Connor (1975) at MIT, code named CAFE, was previously modified for use in Great South Bay by Wong (1981) at the Marine Sciences Research Center (MSRC). Although this model was successfully used in the cited study it suffered from two disadvantages. First, the computer costs required to run this model for the time periods necessary for the simulation of important water quality scenarios in the bar-built estuaries along the southern coast of Long Island are very large. Second, the water quality component of this model had not proved, in preliminary runs, to be readily modified for the studies planned at MSRC. Consequently, an alternate model was sought which would be less costly to run, and which had a water quality component more suitable for application to certain water quality problems under consideration here. Isaji and Spaulding (1981) recently developed computer programs for the solution of the two-dimensional vertically averaged hydrodynamic and transport equations with finite element methods (Galerkin weighted residual technique). An analysis of the code, together with comparison runs made between this newer model and CAFE, showed that the newer model

could be run at much less cost than CAFE, without seriously sacrificing reliability. Also, the water quality component of the Isaji and Spaulding model appeared to be more readily modified for use in the planned studies of the Long Island South shore bays than would be the case for the CAFE model.

The Isaji and Spaulding models are essentially based on the two-dimensional (vertically-averaged) equations of motion, formulated by Pritchard (1971), and the water quality equation, formulated by Christodoulou et al. (1976). The code for these computer programs were written for water bodies along an open coast and have successfully been applied to water quality problems in unbounded open ocean regions. They have not, however, been applied to a bounded system such as a bar-built estuary. There are a number of modifications to be made to the programs in order to be applied to bar-built estuarine systems.

For details on the formulation of the finite element algorithms and the methods for solution of these equations, see the Appendix, Chapters II and III for the hydrodynamic model, and Chapters V and VI for the salinity model.

MODIFICATIONS MADE TO THE MODELS FOR APPLICATION TO GREAT SOUTH BAY

Since the Isaji and Spaulding models had previously been used for open coastal simulations, in which the various model parameters, such as the bottom frictional coefficient and the surface wind stress, could be considered to be invariant in space, use of these models in an bar-built estuary of complex geometry and variable bottom roughness requires some modifications to the hydrodynamic portion of the model to allow such parameters to vary in space. Also, the boundary conditions for a waterway such as Great South Bay involve complexities which also requires modifications to the Isaji and Spaulding models.

The first modification made to the hydrodynamic model was to allow the bottom frictional coefficient, called the Manning coefficient, to vary from element to element. This modification was necessary because bar-built estuaries generally have extensive shallow areas within the waterway but are connected to the ocean by relatively deep inlets. The deeper inlet channels usually have coarser bottom sediments than do the shallow interior regions,

while aquatic vegetation is more likely to cover the bottom in the shallow regions than in the inlet channels. Such differences in bottom characteristics result in spatial variations in values of the bottom frictional coefficient.

The hydrodynamic model was next modified to allow temporal variation in the wind stress on the water surface of the estuary. Adjustment and verification of the model requires comparison of model output with observations of water surface elevation and current velocity over periods of time within which significant variations occur in the distribution of wind stress over the estuary. The local wind blowing over the surface of the Bay does cause a downwind setup of the water surface and affects the current velocities in the Bay. Thus, even though the wind was not simulated in the production runs of the model made to test the effects of Yellow Bar, the inclusion of a time varying wind field was necessary for proper verification of the model.

The other modifications made to the hydrodynamic model involve expanding the options available for the boundary conditions. For the open boundaries, at which sea surface elevations are prescribed, the boundary input conditions were modified to allow either real tide gauge data to be input, or to allow the tide at these open boundaries to be computed using amplitude and phase information for as many tidal constituents as are needed to represent the actual tide at each particular boundary node. Prior to this modification, only a single tidal constituent was allowed to drive the model at the open boundaries. These modifications were necessary in order to verify the model against real data. Both solar and lunar diurnal and semi-diurnal tidal constituents are often important in estuaries, as are shallow water overtides. Also, in most estuaries meteorological tides contribute to significant time variations in the record of the water surface elevations, and these variations contribute to variations in the currents within the waterway.

The model was also modified to allow for more than one open boundary. Great South Bay, like many other bar-built estuaries, communicates with the ocean via more than one open boundary, and this modification was required in order to apply the model to this waterway.

While most drowned river valley estuaries receive the major part of their fresh water input from a single source, the bar-built estuaries along the south shore of Long Island receive fresh water from runoff carried by many small streams, and from ground water inflow. Particularly in Great South Bay, ground water inflow through the Bay bottom constitutes a significant fraction of the total fresh water inflow. Also, the streams which flow into Great South Bay are very narrow compared to the adjacent open Bay. Extending the finite element grid up these small streams to the point where the fresh water inflow could be specified as a boundary condition would require elements having dimensions of only a few meters to a few tens of meters. The length of the time step required to obtain a stable numerical solution to the transient state hydrodynamic equations is proportional to the dimensions of the smallest element in the grid. The cost of running a given simulation of the hydrodynamics and kinematics of the waterway increases rapidly as the number of elements in the grid increases and as the time step decreases. The small size of the elements required to model the small streams which enter Great South Bay would require such a small time step that the computer costs of running any practical simulation of Great South Bay would be prohibitive.

Consequently, a fresh water input boundary condition for the land nodes marking the location of the streams entering Great South Bay was implemented which takes into account both the fresh water which enters the grid element adjacent to each such node from both surface runoff and ground water upwelling from the bottom. The essential features of this procedure are as follows: (a) During each time step of the model run, the volume of fresh water which is calculated to enter the Bay from a given stream and from its companion ground water drainage area during that time step is input to the element just adjacent to the land boundary node marking the mouth of the stream. (b) The model then computes an increment addition to the elevation of the element required to account for the added volume. (c) This added elevation then is reflected in the equation of motion as an increased pressure force resulting from the slope of the water surface away from these source elements, and hence the fresh water input is advected away from the stream mouths in the model simulation in a manner much like that which occurs in the real waterway.

The final modification to the Isaji and Spaulding hydrodynamic model was one which corrected the algorithm which was intended to assure that there is no net flux of water through a land boundary. This condition, called the kinematic boundary condition, was properly implemented in the original model for the case in which the depth of the waterway at the land boundary nodes is the same at each node, at all times during the tidal cycle. In a waterway such as Great South Bay, the tidal mean depths along the shoreline vary with position, as does the tidal amplitude and phasing. These variations resulted in failure of the model to conserve mass due to the loss or gain of water through the solid boundaries. As a result of the correction of the algorithm which implements the kinematic boundary condition, test model runs gave results with very small errors in the mass continuity requirements.

Modifications were also made to the salinity model. These include some relatively straight forward adjustments to the input parameters to take into account the conservative nature of the variable of interest, i.e., salinity, and also our present understanding of the isotropic nature of the process of horizontal eddy diffusion as simulated in this model. Not so straight forward were modification which involved boundary conditions.

At the upstream boundary of the rivers and streams entering an estuary, the boundary condition for salinity should be $S_f = 0$: that is, the salinity of the fresh water source should be set to zero. However, as already noted above, the fresh water streams entering Great South Bay are so narrow that it is not practical to extend the finite element grid up these waterways to the point where the salinity is actually zero. The hydrodynamic boundary conditions applied to the land nodes located at the mouths of the rivers and streams in order to compensate for the fact that the model grid does not extend up into each fresh water source to the point where the salinity can be considered to equal zero, as described in the just previous paragraphs, preclude the setting of the salinity at the nodes marking the mouths of the rivers and streams to a zero value. Instead, the boundary condition for salinity is to prescribe the value of the salinity around the river mouth nodes as that obtained by dilution of the computed salt content of the grid element adjacent to the river mouth by the fresh water discharged into that element. Thus, at each time step the salinity at all nodes is computed using

the advective-diffusive salinity equation, without prescribing a particular value at the river mouth nodes. Then, before making the calculations for the next time step, the computed values of the salinity at each node defining an element adjacent to the mouth of a river or stream is multiplied by the ratio of the volume of that element as computed by the model to the sum of that volume plus the volume of fresh water which is considered to have entered that element during the previous time step. This new "diluted" value of the salinity is then used as the initial value for the next time step.

The salinity must be prescribed in some manner at the open boundaries to the model. However, the salinity cannot be fixed or otherwise prescribed at all times during the tidal cycle at these open boundary nodes, since at least during the period of ebb flow the salinity at these nodes depends on the salinity distribution in the adjacent interior of the model. That is, during the ebb flow period water from the interior of the waterway is advected out past the open boundary nodes, thus carrying the salt content of the adjacent interior waters to these nodes. During the period of flood flow, water from the adjacent open coastal ocean flows in past the open boundary nodes, and at some time during the flood interval the salinity at these boundary nodes becomes equal to the nearly constant (at least for the length of time over which model runs were made for this study) salinity of the nearshore coastal ocean. Therefore the salinity condition implemented for the open boundary nodes is to specify the conditions during the flood interval, but to allow the model to compute the salinity at these nodes during the ebb interval. The specification of the salinity at the open boundary nodes during the flood interval involves the subdivision of this interval into two parts. The first subdivision starts with the last value of the salinity calculated just before the flow reverses from ebb to flood. The salinity at the boundary nodes is then increased linearly, over a set time interval, to the fixed ocean salinity value. This part of the flood interval is called the 'ramping' part. During the second part of the flood interval, the salinity at the open boundary nodes is held constant at the prescribed 'ocean' salinity value. This part of the flood interval is called the 'capping' part. The duration of the ramping part, as well as of the salinity value for the capping part, are determined from salinity data recorded at the mouth of the estuary.

For greater detail on the modifications made to these models see the Appendix, in particular Chapter IV for the hydrodynamic model and Chapter VII for the salinity model.

THE AREA MODELED -- THE GRID FOR GEOMETRIC SIMULATION OF THE BAY AND INLET

The western boundary of the Great South Bay was considered for the purposes of this study to be located at a shallow, constricted cross section near Seaford, about 19 Km westward from Robert Moses Causeway, while the eastern boundary was set at the Smith Point constriction (Fig. 1). Tidal gauge data are available at each of these locations, and generally these constrictions are considered the connecting passages linking Great South Bay with Oyster Bay to the West, and with Moriches Bay to the East.

The southern boundary of the Great South Bay is delineated by the barrier islands which enclose the Bay on the ocean side. Along the southern shoreline of Great South Bay, westward from Robert Moses Causeway, there are many intertidal islands and shallow areas less than 1 m depth, where the circulation is negligible and which could not be handled by the computer program of this model without increasing the friction coefficient beyond reasonable values. This area of the Bay is also marked by very narrow, meandering channels, so that it would be prohibitively expensive to grid with the required fine spatial resolution. For this reason, the southern boundary of the grid simply borders the interior tidal islands and shallow tidal flats immediately adjacent to the barrier islands. Thus, the grid designed for this study, as shown in Fig. 3, consists of 632 nodal points and 992 elements, with the length of the smallest side of an element being 160 m. This minimum grid size is important, since it, in part, sets the time step required to assure numerical stability of the model. The length of the time step sets the cost of running the model -- the smaller the time step, the greater the cost.

DEVELOPMENT OF THE BOUNDARY INPUT DATA FOR THE MODELS

This grid is able to resolve the geometry near the mouths of all the streams along the northern boundary of the Great South Bay, except for Awixa and Tuthills creeks: that is, nodes were located at the mouths of all surface fresh water sources except for these two small creeks, which are so closely and irregularly spaced that they could not be included in the gridding without

distorting the size and shape of the surrounding elements. The stream discharge of the Awixa was included by distributing it between the discharges of Pentaquit and Orowoc creeks, while the discharge of Tuthills was distributed between Corey creek and Patchogue river. The river discharges were estimated on the basis of their surface drainage areas measured from Quadrangle Topographic maps of the U.S. Department of the Interior Geological Survey (scale 1:24,000) using a Compensating Polar Planimeter (PARAGON model 620015). Saville (1962) had estimated that about 95% of the total stream flow is due to ground water discharge, hence, a better distribution of the fresh water input into the Bay would be made by taking the ground drainage area into account rather than the surface drainage. However the scale (1:130,000) of the maps of Water Tables, which cover all the streams of interest (Kozalba, 1975), were too coarse to allow a reasonable estimate for the ground water drainage area. Nevertheless, a linear relationship exists between river discharge and either surface drainage area or ground water drainage area for a given stream as is demonstrated in Chapter X of the Appendix. The analysis given in the Appendix indicates that the ratio of the fresh water flow which enters Great South Bay from a given combined surface and ground water drainage basin to the area of the drainage basin is, on the average, $0.0135575 \text{ (m}^3\text{/s)/Km}^2$, or $1.24 \text{ (ft}^3\text{/s)/mi}^2$.

It is assumed here that this runoff factor determined from the analysis of selected drainage basins is the appropriate run-off factor to be used for the total drainage area of Great South Bay, with minor exceptions to be noted below. As described earlier, not all of the fresh water which enters Great South Bay flows in from surface streams. Some 20 to 35% upwells through the bottom from the ground water reservoirs, mostly from bottom close to the northern shore of the Bay (Bokuniewicz and Zeitlin, 1980). However, it is assumed that the runoff factor of $0.0135575 \text{ (m}^3\text{/s)/Km}^2$, or $1.24 \text{ (ft}^3\text{/s)/mi}^2$, includes both surface runoff and ground water inflow. This runoff factor was applied to the drainage areas of 34 of the 40 fresh water sources to Great South Bay. In the case of six streams for which the discharge vs. drainage area data points fall close to the straight line defined by this runoff factor, the actual measured runoff factors were used. These streams are: Swam river, Champlin, Pentaquit, Santotogue, Orowoc, and Awixa creeks. As shown in Table 1, these assumptions results in a computed long time average fresh water

inflow to Great South Bay of $13.1 \text{ m}^3/\text{s}$, which agrees very well with that of $13.5 \text{ m}^3/\text{s}$ estimated by Saville (1962).

Most of the field data used for driving the models at the boundaries, and for adjustment and verification of the models, were collected during the New York Sea Grant sponsored Great South Bay project which was conducted by the Marine Sciences Research Center during the period May, 1979 to October, 1970. Fischer and Porter model 1550 tide gauges were deployed at the West Islip, Fire Island Coast Guard Station, Captree Island, Sailor Haven and Timber Point (Fig. 4) during the full period of the survey. These instruments record sea level elevation on punched paper tape at 15 minute intervals. Additional sea level records from stations to the west and to the east of Great South Bay were available through various federal and local agencies. Hourly elevations at Seaford (Fig. 4) were obtained from the town of Hempstead, Department of Conservation and Waterways, in the form of analogue signals recorded by Bristol model 2L681-16-1A bubbler type liquid level gauges. Sea level elevations at Smith Point (Fig. 4) were obtained from the Suffolk County Department of Public Works, Division of Waterways in the form of analogue signals recorded by Bristol model 1G3X628-15 bubbler gauges. An ENDECO 174 current meter was maintained for 15 months in the mid-bay area (Fig. 1). Current meters (ENDECO 174's and ENDECO 105's) were also deployment for a period of approximately one month at other locations as shown in Figure 4. All current meters were deployed at a depth of 1 m. The ENDECO 174 current meter records current speed, direction, temperature and conductivity at two minutes intervals on magnetic tape: the ENDECO 105 current meter records speed and direction of the current at 30 minutes intervals on film. Records of hourly wind speed and direction from the weather station at Tiana Beach (Fig. 1) were obtained through the Division of Meteorology at Brookhaven National Laboratory. These measurements were made with an Aerovane model 120 Anemometer. Salinity data were calculated using the temperature and conductivity recorded by the ENDECO 174. Unfortunately there were no calibrations for the temperature and conductivity channels of these current meters. So, the time histories and spatial distributions of salinity from these meters can only be used to study time variations in relative values, but not the 'absolute' values of the salinity. All the tide, current, wind velocity and salinity

data used for this study were filtered using a Lanczos filter with a half power point of 3 hours to eliminate high frequency fluctuations.

VERIFICATION OF THE MODELS

Before exercising the models on the complex grid used to simulate the geometry of Great South Bay, a number of runs were made using simpler grids in order to test the model for agreement with analytical results which are obtainable under some simplifying assumptions, and to determine the degree that the models satisfy the requirement for conservation of mass and salt.

In the first verification test the hydrodynamic model was used to simulate a standing tidal wave in a simple rectangular shaped basin of constant depth, open to the ocean at one end and closed at the other end and along the sides. A single harmonic (M_2) tide was used to force the system at the open boundary. Coriolis, wind stress and bottom friction forces were not included in this simulation. Under these conditions a standing wave is set up in the basin for which there exists an exact analytical solution. Figure 5 shows a comparison of the analytical and numerical results for an interior node located in the center of the basin. It is clear from this comparison that the numerical model gives quite accurate results for this simple case.

Tests were then made on more complex cases for which no analytical solutions exist, in order to determine the accuracy of the model from the standpoint of conserving mass. In all these tests all of the terms in the momentum equation were included. These tests included the following:

(a) A rectangular shaped grid which is opened along one face, and closed along the other three faces. A single harmonic (M_2) tide was input at the open boundary. This grid was exercised with and without an inflow through the landward boundary to simulate a river input. Computations were made of the tidal mean volume flux through each section along the length of the simulated waterway. In the case of no inflow through the landward boundary, the tidal mean flux through each section should equal zero. In the case of the simulation of a river inflow, the volume flux through each section should equal the volume rate of inflow through the landward boundary. In all of these tests the model output closely matched the expected value.

(b) A series of tests were made on a trapezoidal shaped grid with three open boundaries. This grid has a superficial appearance of a simplified Great South Bay. The model was forced with a single harmonic (M_2) tide at each open boundary, with the relative amplitudes and the phase differences of the forcing tide at each opening similar to that which exists at the three openings of Great South Bay. The hydrodynamic model was run on this grid for conditions of constant depth and spatially varying depth, without any fresh water inflow, and also with a steady fresh water inflow through the upper land boundary, that is, through the boundary which would correspond, in this simplified simulation, to the north shore of Great South Bay. The fresh water inflow was input as a normal flux per unit length along this boundary. Values of the net tidal mean flux through several cross sections in the throats leading to the three open boundaries were computed, and compared to the expected values. These tests showed that, even for these more complex cases, the errors in the model conservation of mass are quite small, and acceptable for the purposes of this study.

(c) The same grid and open boundary tidal driving as described in (b) above was again simulated, with a fresh water input using the modified algorithm developed to account for the fact that, from a practical standpoint, the small fresh water streams cannot be geometrically simulated in the model. This test showed that this algorithm over computes the input of fresh water, and that a constant factor, having a value somewhat over unity, must be used as a multiplier for the expected fresh water input. This factor appears, however, to be a constant for a given geometry and tidal forcing.

A detailed description of these model verification tests, including an explanation for the correction factor which must be applied for the algorithm for input of the fresh water as a volume source into the elements adjacent to the river mouth nodes, is given in Chapter VIII of the Appendix.

A test was also run to determine how well the salinity model conserved the mass of salt. In this test a long rectangular shaped estuary, driven by a single component (M_2) tide at the ocean end and a fresh water inflow at the landward end, was simulated. The hydrodynamic model was run to steady state for this grid and boundary forcing, and the tidally varying velocity distribu-

tion was then input to the salinity model. The salinity boundary conditions at the ocean end were those described earlier in the section entitled "Modifications Made To The Models For Application To Great South Bay". The salinity model was then run for a period of 87 tidal cycles to attain as near a steady state condition as was practical.

Salt continuity in this case requires that the diffusive flux of salt through any cross section be equal in magnitude but opposite in sign to the advective flux of salt through that cross section. Computations of the ratio of the tidal mean advective and diffusive salt flux for the 49 cross sections in this simulated waterway were made. The results of this test show that the coupled hydrodynamic - salinity model adequately conserves salt. Chapter IX of the Appendix gives a detailed description of this test.

After completion of these tests using the simplified grids as described above, calibration runs of the model using the complex grid simulating the geometry of Great South Bay were made for the purpose of determining the values of the Manning coefficient and eddy viscosity coefficients of the momentum equation, and the eddy diffusivity coefficients of the salinity equation, which resulted in a model simulation of values of the hydrodynamic variables, i.e., the time varying water surface elevation, the two horizontal components of the vertical mean velocity, and the salinity, at positions close to the points at which observed data were obtained. To calibrate the hydrodynamic model, 10 semidiurnal lunar tidal cycles (from 10:00, 16 September, 1980 to 14:00, 21 September, 1980), were selected from our data set for the open boundary conditions at Seaford, Smith Point, and Fire Island Coast Guard Station. The absolute levels of these tide gauges referenced to a defined datum were not known. Consequently, as a first order approximation the individual record mean levels for all three gauges were assumed to lie on the same absolute level surfaces. The data from each station were then referenced to local MLW at Fire Island Coast Guard Station.

A first calibration run was made in which the grid at the entrance to Fire Island Inlet was truncated to the Fire Island Coast Guard Station because no recorded tide data was available at the actual ocean entrance location. Wind velocity data used to compute wind stress during the calibration period

was obtained from the weather station at Tiana Beach. The river discharge used during this period for each of the simulated fresh water sources is shown in Table 1.

The observed tide gauge data for the calibration period at West Islip, Timber Point, and Sailor Haven, are shown in Figure 6, and the observed East-West and North-South components of the current velocity at Mid-Bay, Smith Point and Fire Island Coast Guard Station, are shown in Figures 7 and 8. The model solutions shown in these figures are for a constant Manning coefficient of $0.0521 \text{ m}^{-1/3}/\text{s}$ ($0.035 \text{ ft}^{-1/3}/\text{s}$) over the entire bottom of Great South Bay, and, for a constant eddy viscosity of $250 \text{ m}^2/\text{s}$. It is clear that except for the initial spin-up of the model, the comparisons between the observed and simulated surface elevation in the interior of the Bay show good agreement both in phase and amplitude of the sea surface elevation (Fig. 6). As time progresses, the model acquires 'memory', improving the agreement except for Timber Point. This was because the tidal gauge at Timber Point was installed in a small bay inside of a narrow inlet on the north shore of the Bay. As a result, the recorded data is significantly attenuated relative to a location just outside the small harbor where the computed data apply. The ability of the program to reproduce the correct amplitude and phase of the velocity inside the Bay is shown in Figures 7 and 8. The accuracy on the reproduction of the velocity by the model increases as the period for the simulation increases. It should be noted that at the low velocities characteristic of the mid Bay location, the calibration accuracy of the current meters decreases. There is also evidence that the rotor on the current meter at Smith Point suffered some periods of fouling, which appeared to be cleared from the rotor during the last two tidal cycles of the simulation. Taking these facts into account, there is reasonable agreement between the observed and computed velocities. Better agreement between the model results and the data recorded can be achieved by locally adjusting the Manning coefficient and the eddy viscosity. However, for the purpose of our study, the accuracy obtained is satisfactory. Thus, no further effort was made to improve the calibration, although it was noted that the model results are much more sensitive to the Manning coefficient than to the eddy viscosity.

A second calibration was necessary in order to extend the open boundary at Fire Island Inlet farther seaward from Yellow Bar. The new location of the open boundary was placed at the Breakwater (Fig. 1) where the sea surface elevation is not affected by the Inlet. Because there were no tidal data available at the Breakwater during the calibration period, the tide used as open boundary condition at this location was generated from that at Fire Island Coast Guard Station, modifying its range by the ratio (1.25/0.58) of the tidal mean range at Breakwater and Fire Island Coast Guard Station, and its phase by the mean lag of high and low water (27 min) between these locations obtained from the Tide Tables of the U.S. Department of Commerce (1979). The hydrodynamic model was then run again for the same time period and conditions of surface wind stress and tides at Seaford and Smith Point used during the first calibration run. In this way, reproduction of the tide at Fire Island Inlet Coast Guard Station was achieved with good agreement (Fig. 9). A different value for the Manning coefficient was applied ($0.013 \text{ ft}^{-1/3}/\text{s}$) from Breakwater up to the Fire Island Coast Guard Station, than that used for the interior of the Bay ($0.035 \text{ ft}^{-1/3}/\text{s}$), because of the relative smooth, vegetation free bottom of the inlet channel compared to the rough vegetated bottom of the interior of the Bay.

It was not possible to calibrate the salinity model as accurately as the hydrodynamic model because of the lower quality of the available salinity data at the boundaries and in the interior of the Bay. As a result, the same value ($100 \text{ m}^2/\text{s}$) for the eddy diffusivity found during the mass conservation test of the salinity model was used for the Great South Bay salinity simulation.

PRODUCTION RUNS OF THE MODEL -- TEST CONDITIONS WITH AND WITHOUT YELLOW BAR

The hydrodynamic model was run with a simple harmonic semidiurnal component (M_2) of the tide, with a range of 1.65 m, 0.46 m and 0.54 m for Breakwater, Smith Point and Seaford, respectively, and phase differences relative to Breakwater, of 2.2 hr and 3.7 hr for Smith Point and Seaford, respectively. The tides were leveled (82.5 cm) with reference to local mean low water at Breakwater. The ranges and lags of these tides were taken from our data set, and they represent typical spring tide conditions. The model was run with and without Yellow Bar, until it reached steady state (around 12 tidal cycles, beginning from 'cold start' initial conditions; i.e., the velocities were

initially set to zero and the water level was set uniformly to mean tide level. The fresh water discharges used were those given in Table 1 (referred to here on as medium river flow conditions). However, the procedure used to simulate the fresh water input as a volume source to the elements adjacent to the river mouth, as described earlier in this report and in Chapters IV and VII of the Appendix, results in a slight difference between the tidal average fresh water input seen by the model and that expected based on the volume added to each adjacent element during each time step. The reason for this difference is related to variations in amplitude and phase at the three nodes of a given element. The fresh water discharge actually simulated in the model runs are determined after the runs are completed, based on the net difference in the tidal average discharges through the three open boundaries. On this basis, the total fresh water discharge for the spring tide simulation without the Yellow Bar, was $12.3 \text{ m}^3/\text{s}$, which is only 6% less of the mean shown in Table 1. The scheme used to prescribe the fresh water input to the Bay from the rivers is, to some extent, dependent on tidal range and phase at the river boundary nodes which differ somewhat with Yellow Bar as compared to the case without Yellow Bar. As a result, the river discharge for the spring tide simulation with Yellow Bar was $11.9 \text{ m}^3/\text{s}$, or 3% less than for the simulation without Yellow Bar.

Once the hydrodynamic model was exercised, the resultant surface elevation and velocity fields were used to simulate the salinity distribution in the Great South Bay. However, the open boundary for the salinity model at Fire Island Inlet was moved into Democrat Point (Fig. 19), because the shoal areas in the eastern part of the entrance of the Inlet near Breakwater produced instabilities in the computed salinities. The prescribed salinities at the open boundaries of the Bay, for the capping interval, could not be obtained from our uncalibrated salinity data. They were, however, estimated from the average of all salinity data at stations close to the location of the open boundaries of the Bay collected by the Suffolk County Health Department: they are 30.6 ‰, 29.6 ‰ and 33.18 ‰ for Seaford, Smith Point and Fire Island Inlet, respectively. The duration of the ramping interval was estimated on the basis of the shape of the salinity data for Smith Point and Fire Island Inlet with the values being 42% and 38% of the M_2 cycle, respectively. For Seaford, for which salinity data was not recorded, it was assumed to be

half of the flooding interval (25% of the M_2 cycle). The model was also run until a steady state was achieved. The number of tidal cycles to reach the steady state for the salinity model depended on the given initial salinity distribution.

The tidal and salinity boundary conditions at the three open boundaries used in these model runs are summarized in Table 2.

THE RESULTS OF THE HYDRODYNAMIC AND SALINITY SIMULATIONS -- WITH AND WITHOUT YELLOW BAR

The spatial velocity field simulated for the Great South Bay is shown in Figures 10 and 11. The former represents maximum flood relative to Democrat Point (open boundary for the salinity model) with and without Yellow Bar, and the latter is for maximum ebb. While the scale of these figures as reproduced here makes it difficult to readily see differences in the flow patterns in the two cases, the original, large, computer generated plots clearly show the attenuation of the velocity due to the presence of Yellow Bar. This attenuation is more marked in the Inlet, around Yellow Bar, than inside the Bay. There is an increase in the magnitude of the velocity at the constriction formed by Yellow Bar. This results from the requirement of continuity. Inside the Bay, the numerical output of the model shows that there is a decrease in magnitude of the velocity field when Yellow Bar is part of the geometry of the Inlet. However, this decrease is not clearly seen even in the original large plots because the magnitude of the velocity field with and without Yellow Bar is very low (2 cm/s).

We would expect that if the hypothesis concerning the effect of changes in the geometry of Fire Island Inlet, as described in the Introduction to this report, were to be correct, then there should be a difference in the tidal ranges within the Bay and in the peak flood and ebb flows and in the tidal mean discharges through the three open boundaries. The model results as given in Table 3 indicate that a dredging project of the magnitude of the removal of Yellow Bar, at least as simulated in these model runs, would result in a significant increase in the tidal ranges in the Bay. Table 4 also shows that the peak flood and ebb flows, and also the tidal average discharge, through Fire Island Inlet as computed by the model are significantly greater without

Yellow bar than with Yellow Bar. This table also shows that, although the removal of Yellow Bar had little effect on the peak flood and ebb flows through the other two open boundaries to Great South Bay, the tidal average discharge through these openings as computed without Yellow Bar were significantly larger than the values computed with Yellow Bar.

The spatial distribution of the tidal mean salinity simulated for the Great South Bay without Yellow Bar, with Yellow Bar, and the differences for spring tide conditions and for a fresh water inflow of about $13.1 \text{ m}^3/\text{s}$ are shown in Figures 12 and 13. The salinity field shows a tilting of the isohalines to the west on the north shore of the Bay, and to the east on its south shore, for the eastern part of Great South Bay. In the western Bay, the isohalines tilt the opposite way. This lateral gradient in salinity, with the higher salt content to the right of the direction of non-tidal flux of water (to the east in the east part and to the west in the west part of the Bay) can not be attributed to earth's rotation, since it is exactly opposite to what should be expected. Instead, it is more related to the fresh water distribution along the north shore of the Bay which produces more dilution of the salinity in those areas than on the south shore. The differences in salinity show a radial change around the Yellow Bar region with maximum gradients close to the Yellow Bar and with a weak gradient inside the Bay. There is a bay-wide average reduction of 1.35 ‰ in the salinity. In the Inlet close to the Yellow Bar, the displacement of the isohalines with and without Yellow Bar is small even though the isolines change in magnitude bay as much as 2 ‰ . This situation is different inside the Bay. There, the isohalines also change quantitatively by about 2 ‰ but their position shifts about 5 Km when Yellow Bar is removed.

The above simulations were repeated using only 41% of the river discharge shown in Table 1. This was done to study the effect of Yellow Bar on the salinity distribution within the Bay under an extreme low river flow condition. The hydrodynamic results for these simulations show almost the same values as those obtained in the previous simulation and they have not been reproduced here. These results were expected since, even for the total river discharge variation of $13.12 \text{ m}^3/\text{s}$, the total flooding flux across the mouth of

Fire Island Inlet is about 100 times larger than the fresh water discharging from the north shore into Great South Bay.

The spatial distribution of the tidal mean salinity simulation for the Great South Bay without Yellow Bar, with Yellow Bar, and the differences for spring tide conditions and low river flow of about $7.1 \text{ m}^3/\text{s}$ are shown in Figures 14 and 15. The characteristics described for the salinity distributions and the differences obtained for the case of medium river flow apply to this case of low fresh water inflow, except that now there is only a reduction of 0.85 ‰ in the bay-wide average due to Yellow Bar.

To study the degree that variations in tidal range may influence the effects of Yellow Bar on the salinity distribution within the Bay, the two previous simulations for medium and low river flow were repeated using tidal ranges at the three open boundaries characteristic of neap tide. The tidal ranges prescribed at Breakwater, Smith Point and Seaford were 0.65 m , 0.22 m and 0.26 m , respectively. The lag in the surface elevation for these locations were the same as those prescribed for the spring tidal range case.

Because the hydrodynamic solutions for the neap tidal range show the same characteristics as for the spring tidal range solutions except that now the amplitude of elevations and velocities were reduced, they are not reproduced here. The spatial distribution of the tidal mean salinity simulated for the Great South Bay without Yellow Bar, with Yellow Bar, and its differences, for the medium river flow, are shown in Figures 16 and 17, and for the low river flow, in Figures 18 and 19. For the case of medium river flow (neap tidal range) there was a reduction in the bay-wide average salinity of 0.54 ‰ produced by Yellow Bar, while for the low river flow, this reduction was only 0.28 ‰ .

SUMMARY AND CONCLUSIONS

An hydrodynamic and a salinity model, originally developed by Isaji and Spaulding (1981) was modified for use in Great South Bay. The hydrodynamic model was tested in a hypothetical waterway having simple geometry, for a standing tidal wave for which an exact solution exists. A number of trial runs were also made in hypothetical waterways of increasing geometric complex-

ity to determine the accuracy of these models in conserving mass and salt. Adjustment and verification runs were also made using a grid which closely simulated the complex geometry of Great South Bay. Model results were compared with observations of water surface elevation (tide gauge records) and with water velocity data obtained from current meters deployed at a number of locations in Great South Bay. These trial runs verified that the model can produce results of adequate accuracy for the purposes of this study.

These models were then run on the grid for Great South Bay which was configured to match the geometry of Fire Island Inlet for two different conditions. One of these conditions represented the bathymetry of the Inlet prior to April, 1970, at a time when a shoal area, called Yellow Bar, located about 1 km (3300 feet) eastward from Robert Moses Bridge, extended roughly northwestward from Fire Island to form a very restricted cross section. Our interpretation of the bathymetric data available to us for that time indicates that the cross section at this location had a mean Low Water area of 2283 m². This was the most restrictive section along the length of the Inlet.

The other condition tested represented the bathymetry of Fire Island Inlet after August, 1970. During the interval April-August, 1970, 1.7 million cubic yards of sand were dredged from Yellow Bar by the Long Island Park Commission, State of New York, in order to provide fill for the construction of a parking area at Robert Moses State Park on Fire Island. According to our interpretation of the available bathymetric data for that time, the removal of Yellow Bar resulted in a cross-sectional area at that location of 6812 m². This change in cross-sectional area from 2283 m² to 6812 m² should not be interpreted as indicating the change in the area of the critical 'throat' cross section in the Inlet. After the removal of Yellow Bar, an extended reach located some 2600 m west of the location of Yellow Bar became the critical 'throat' cross section, with a cross sectional-area of 3685 m².

Thus the removal of Yellow Bar resulted in a relocation of the critical 'throat' cross section, and an increase in the critical cross-sectional area from 2283 m² to 3685 m².

Note that our simulation of Yellow Bar may have somewhat over estimated its constrictive effect on flow through Fire Island Inlet, in that we did not

provide for flow over the Bar during the period when the water surface elevation was above mean tide level.

The Bay-wide average values of salinity, and of salinity differences with and without Yellow Bar, are shown in Table 5 for the various conditions simulated in these production runs of the model. Assuming that the average of the Spring Tide and Neap Tide results represent a good estimate of the situation under mean tide conditions, then the Bay-wide average salinity increase due to the removal of Yellow Bar under mean tide conditions is 0.94 ‰ for median fresh water inflow. This increase is associated with an increase in the cross-sectional area of the critical 'throat' cross section from 2283 m² to 3685 m². Hence the ratio of the incremental increase in Bay-wide average salinity to the increase in critical cross sectional area equals 0.67 ‰ per 1000 m² change area.

Note that either with or without Yellow Bar, there is a difference in the computed Bay-wide average salinity for median fresh water inflow as compared to low fresh water inflow, with higher salinities for the lower fresh water inflows. For the case without Yellow Bar (i.e., for existing conditions), the ratio of the incremental change in Bay-wide mean salinity to the incremental change in fresh water input amounts to 0.228 ‰ per m³/s for spring tide conditions and to 0.420 ‰ per m³/s for neap tide conditions, or an average of 0.324 ‰ per m³/s. The Southwest Sewer District project involves the collection of water which would have ultimately entered Great South Bay as ground water. After treatment this water is discharged directly to the ocean. The design flow for the Southwest Sewer District Treatment Plant is approximately 30 MGD, which corresponds to 1.314 m³/s. Our model results then suggest that the diversion of fresh water from Great South Bay by the Southwest Sewer District would, at design flow, result in an increase in the Bay-wide average salinity of some 0.43 ‰.

TABLE 1

ESTIMATION OF THE TOTAL STREAM DISCHARGE INTO THE GREAT SOUTH BAY.

NAME	TOTAL SURFACE DRAINAGE AREA (Km ²)	TOTAL STREAM DISCHARGE (m ³ /s)
Massapequa Creek	104.4588	1.42
Jones Creek	7.5624	0.10
Carman Creek	6.5012	0.09
Narraskatuch Creek	3.4122	0.05
Amityville Creek	10.8604	0.15
Woods Creek	2.3053	0.03
Howell Creek	2.4394	0.03
Great Neck Creek	3.4939	0.05
Strongs Creek	3.5035	0.05
Neguntatogue Creek	5.8417	0.08
Santapogue Creek	20.1470	0.27
West Babylon Creek	3.8727	0.05
Carlls River	116.1698	1.57
Sampawans Creek	64.3560	0.87
Willetts Creek	7.7551	0.11
Trues Creek	2.4784	0.03
Thompsons Creek	1.4563	0.02
Penataquil Creek	14.1389	0.19
Awixa Creek	6.6840	0.07
Orowoc Creek	28.7445	0.38
Champlin Creek	21.5705	0.29
Connetquot River	94.4261	1.48
Ludlows Creek	8.2188	0.11
Indian Creek	5.8123	0.08
Green Creek	18.8441	0.26
Brown Creek	35.6637	0.48
Homans Creek	2.2355	0.03
Namkee Creek	1.3192	0.02
Stillman Creek	1.4629	0.02
Corey Creek	2.4784	0.03
Tuthills Creek	7.1576	0.10
Patchogue River	38.9779	0.53
Little Creek	4.4278	0.06
Swam River	23.3567	0.38
Mud Creek	13.1753	0.18
Abets Creek	6.4522	0.09
Hedges Creek	5.5674	0.08
Howells Creek	2.4294	0.03
Beaverdam Creek	9.4302	0.13
<u>Carmans River</u>	<u>230.9388</u>	<u>3.13</u>
40 STREAMS	950.1263	13.12

TABLE 2
MODELING BOUNDARY CONDITIONS

BOUNDARY LOCATION	SPRING TIDE RANGE (m)	NEAP TIDE RANGE (m)	FLOOD CAP SALINITY
Fire Island Inlet Breakwater Democrat Pt.	1.650	0.647	33.18
Smith Point	0.460	0.220	29.60
Seaford	0.544	0.350	30.60

TABLE 3
EFFECTS OF YELLOW BAR ON GSB TIDAL RANGES

LOCATION	SPRING TIDE RANGES (m)		
	WITH YELLOW BAR	WITHOUT YELLOW BAR	PERCENT INCREASE
Robert Moses (North)	0.160	0.288	80.0
Brown Pt. (Sayville)	0.178	0.297	66.9

LOCATION	NEAP TIDE RANGES (m)		
	WITH YELLOW BAR	WITHOUT YELLOW BAR	PERCENT INCREASE
Robert Moses (North)	0.075	0.134	78.7
Brown Pt. (Sayville)	0.086	0.146	69.8

TABLE 4

EFFECTS OF YELLOW BAR ON TIDAL FLOWS AND TIDAL AVERAGE DISCHARGES
THROUGH THE THREE OPEN BOUNDARIES TO GREAT SOUTH BAY

	VOLUME RATE OF FLOW - M ³ /SEC	
	<u>WITH YELLOW BAR</u>	<u>WITHOUT YELLOW BAR</u>
FIRE ISLAND INLET		
Peak Flood Flow(In)	2395	4100
Peak Ebb Flow(Out)	2690	3250
Net Discharge	52.9(In)	106.5(In)
SMITH POINT		
Peak Flood Flow(In)	372	336
Peak Ebb Flow(Out)	394	393
Net Discharge	36.2(Out)	64.2(Out)
SEAFORD		
Peak Flood Flow(In)	434	277
Peak Ebb Flow(Out)	458	390
Net Discharge	28.6(Out)	54.7(Out)

TABLE 5

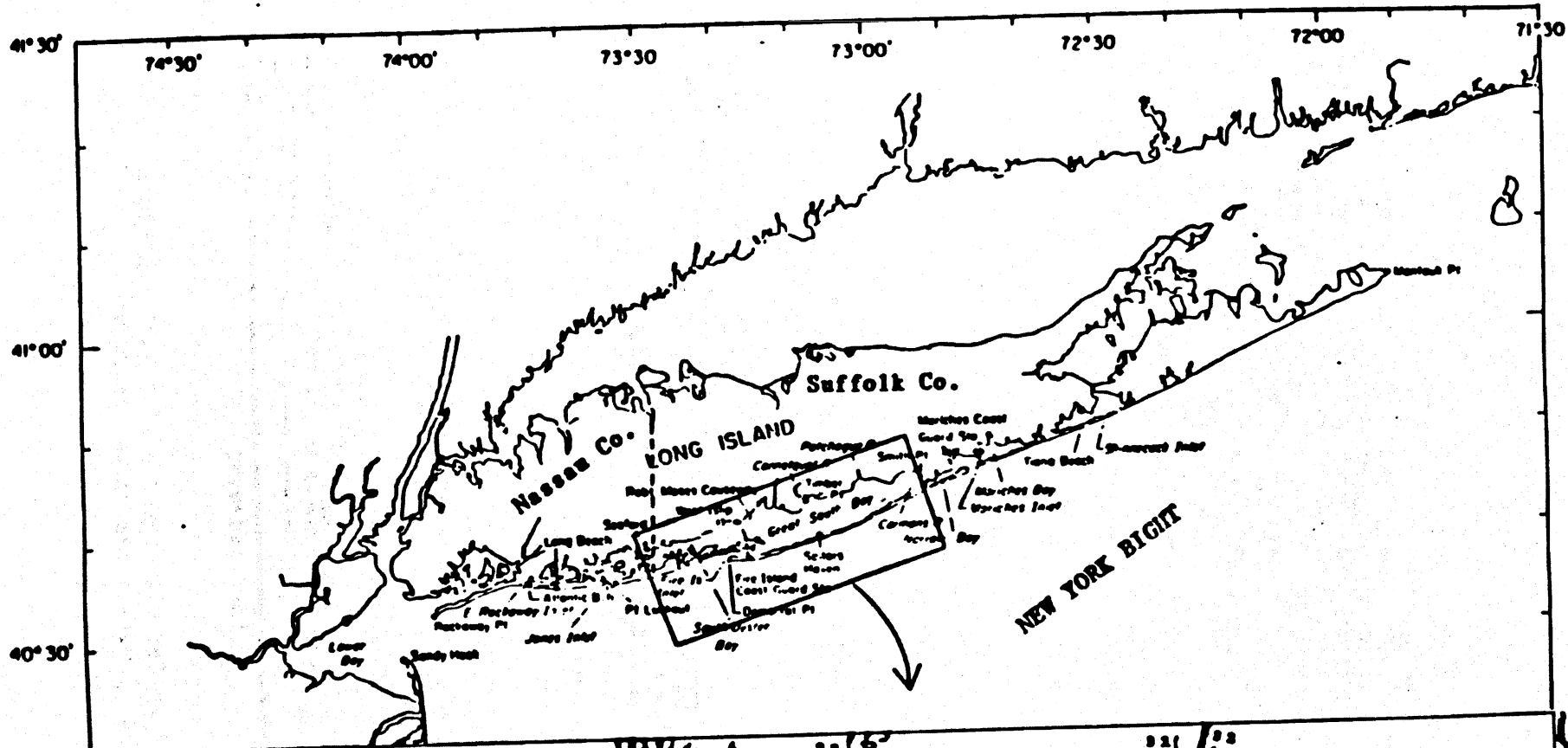
RESULTS OF SALINITY MODEL RUNS

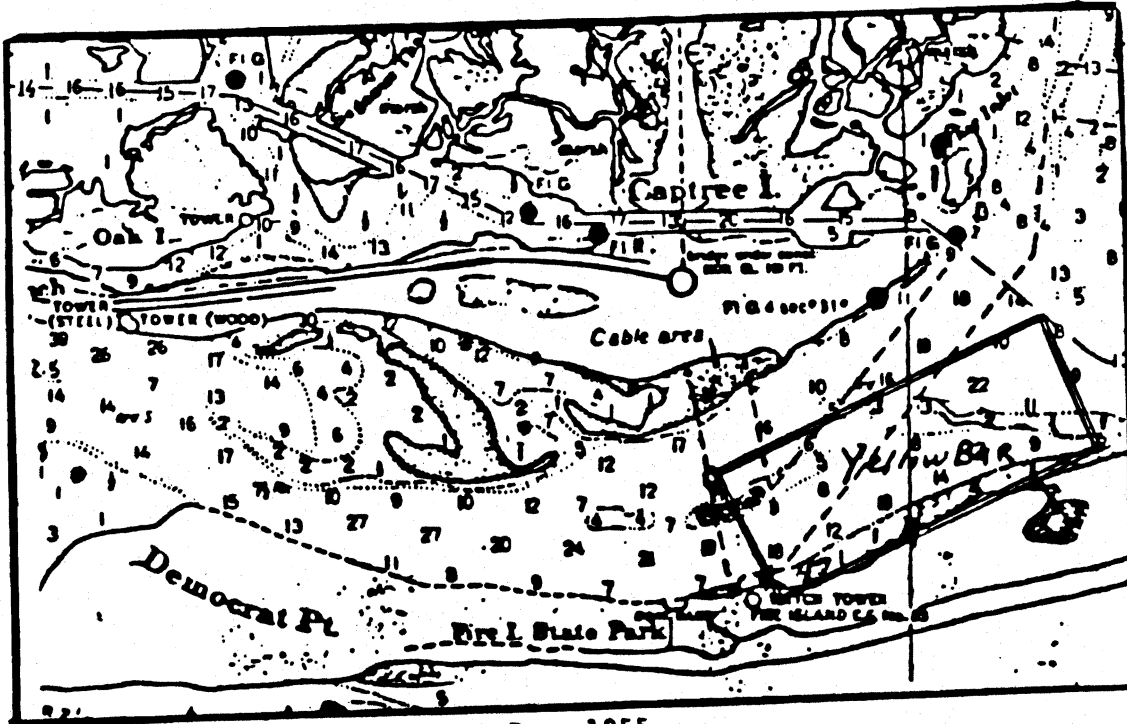
BAYWIDE MEAN SALINITIES

<u>TIDE</u>	<u>FRESH WATER INFLOW</u>	<u>WITH YELLOW BAR</u>	<u>WITHOUT YELLOW BAR</u>	<u>SALINITY INCREASE</u>
SPRING	MEDIAN	26.16	27.51	1.35
NEAP	MEDIAN	25.63	26.17	0.54
SPRING	LOW	27.80	28.65	0.85
NEAP	LOW	27.99	28.27	0.28

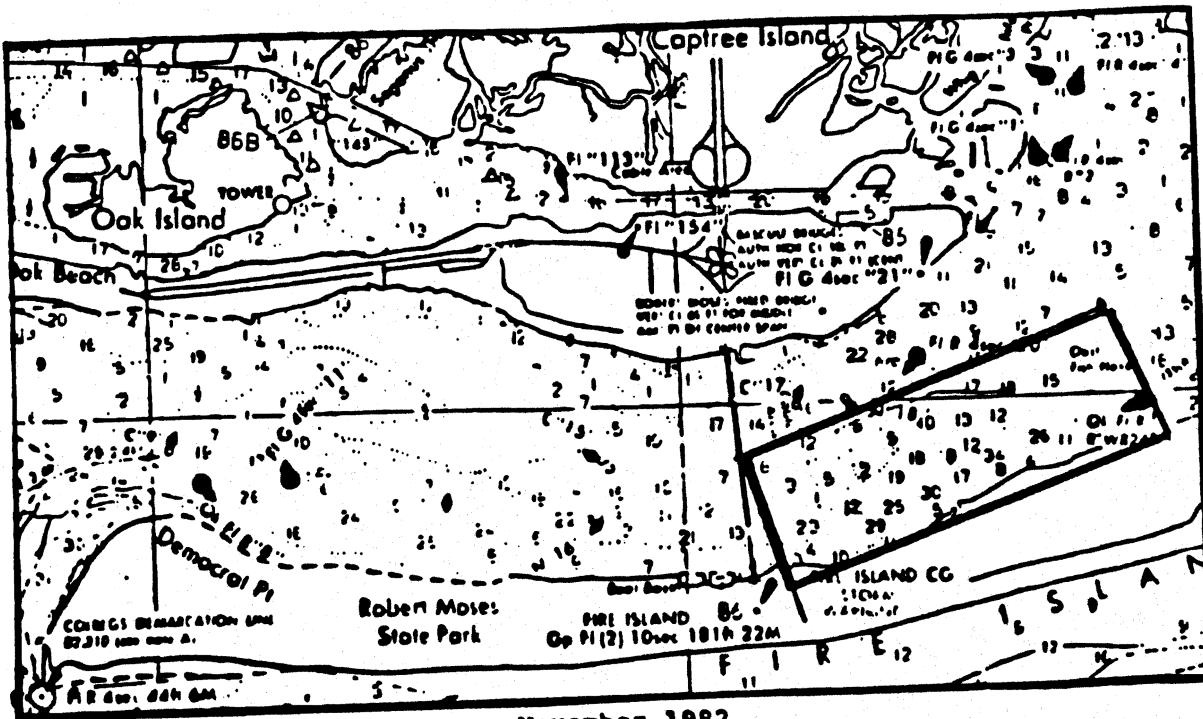
Figure 1. Location map for Great South Bay, New York (map scale for Great South Bay 1:240,000):

- | | |
|-------------------------|-----------------------|
| 1.- Massapequa Creek | 21.- Champlin Creek |
| 2.- Jones Creek | 22.- Connetquot River |
| 3.- Carman Creek | 23.- Ludlows Creek |
| 4.- Narraskatuch Creek | 24.- Indian Creek |
| 5.- Amityville Creek | 25.- Green Creek |
| 6.- Woods Creek | 26.- Brown Creek |
| 7.- Howell Creek | 27.- Homans Creek |
| 8.- Great Neck Creek | 28.- Namkee Creek |
| 9.- Strongs Creek | 29.- Stillman Creek |
| 10.- Neguntatogue Creek | 30.- Corey Creek |
| 11.- Santapogue Creek | 31.- Tuthills Creek |
| 12.- West Babylon Creek | 32.- Patchogue River |
| 13.- Carlls River | 33.- Little Creek |
| 14.- Sampawans Creek | 34.- Swam Creek |
| 15.- Willetts Creek | 35.- Mud Creek |
| 16.- Trues Creek | 36.- Abets Creek |
| 17.- Thompsons Creek | 37.- Hedges Creek |
| 18.- Penataquil Creek | 38.- Howells Creek |
| 19.- Awixa Creek | 39.- Beaverdam Creek |
| 20.- Orowoc Creek | 40.- Carmans River |





June 1955



November 1982

Figure 2. Fire Island Inlet with Yellow Bar (above) and without Yellow Bar (below). Scale 1:50000.

Figure 3. Finite Element Grid for Great South Bay (scale 1:250000)

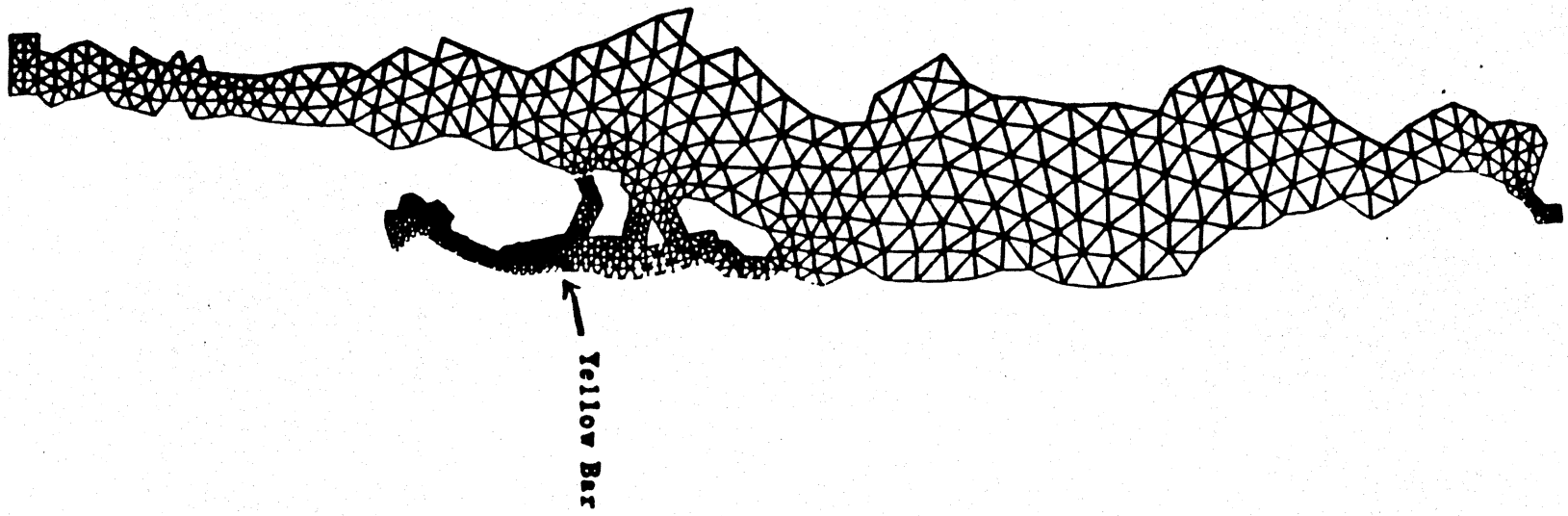
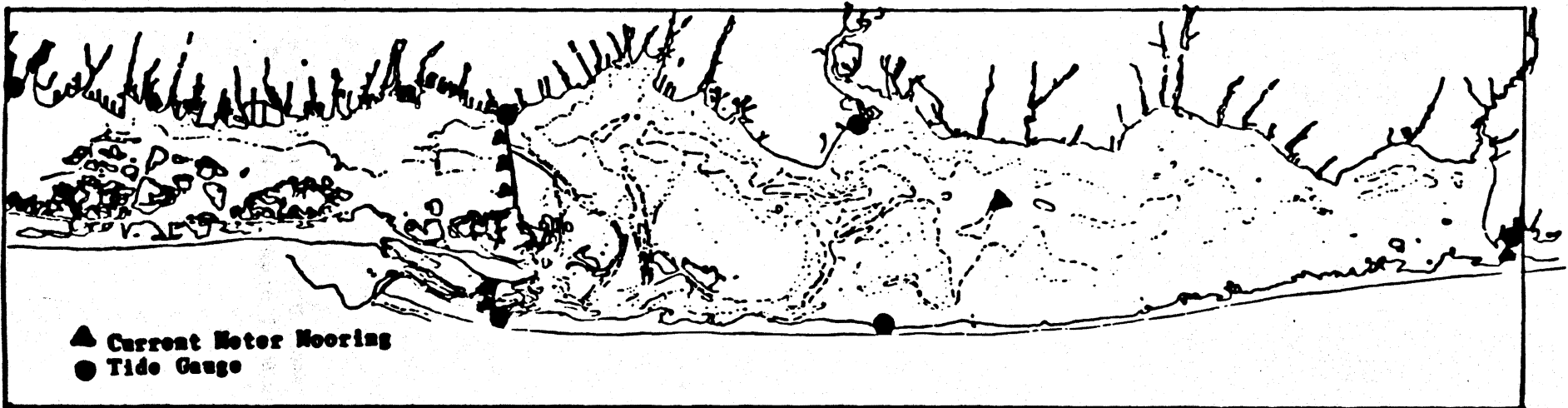


Figure 4. Position of instruments within Great South Bay.



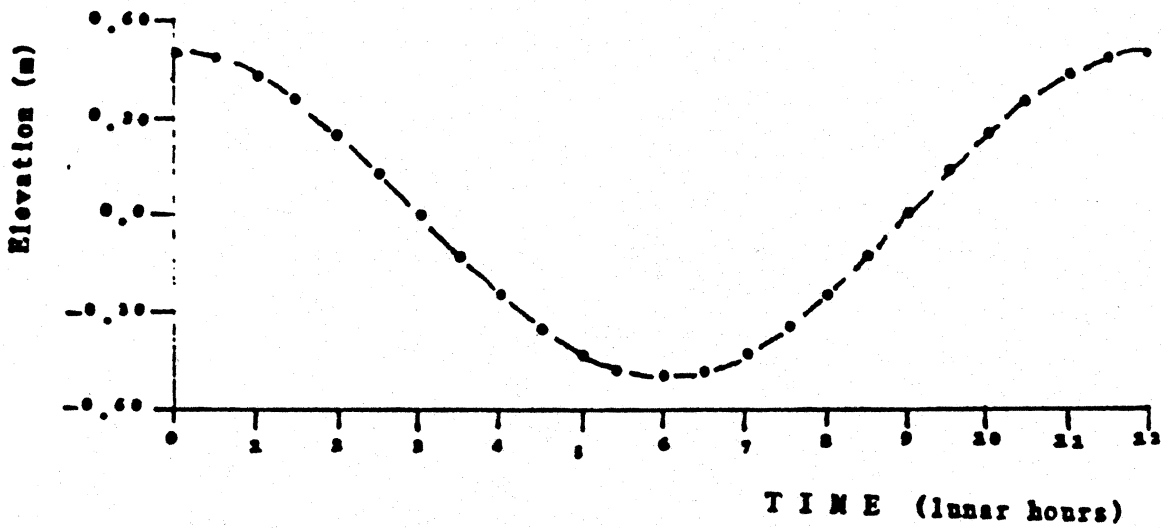
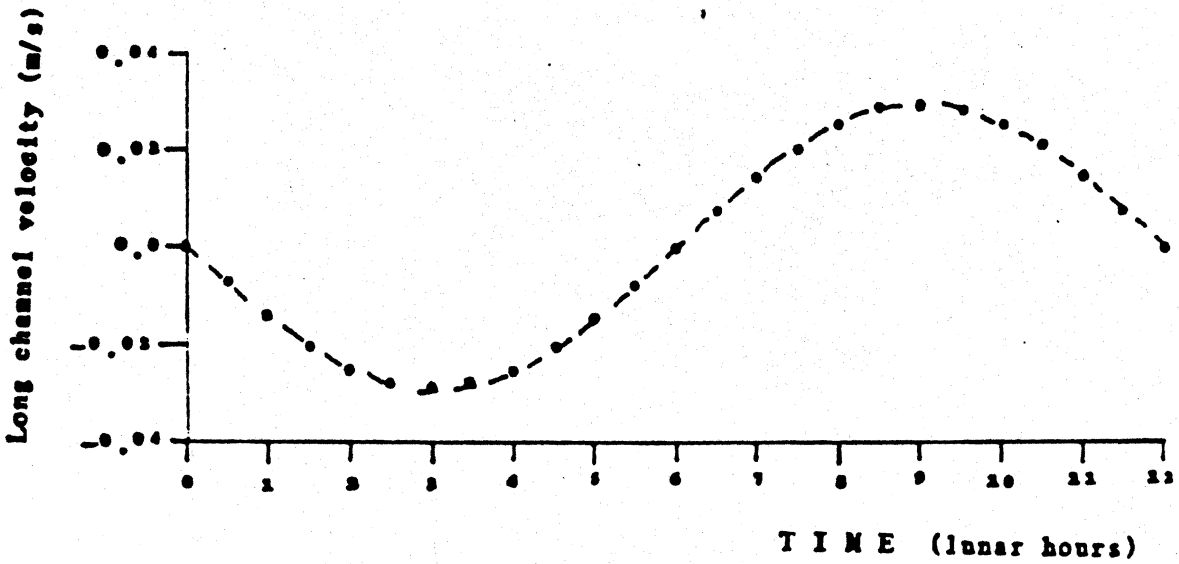


Figure 5. Analytical (•••) and numerical (---) solutions for a standing wave in middle of of the rectangular grid.

Figure 6. Observed surface elevation data (dashed line) and model computations (solid line) during the first calibration at Sailor Haven, Timber Point and West Islip.

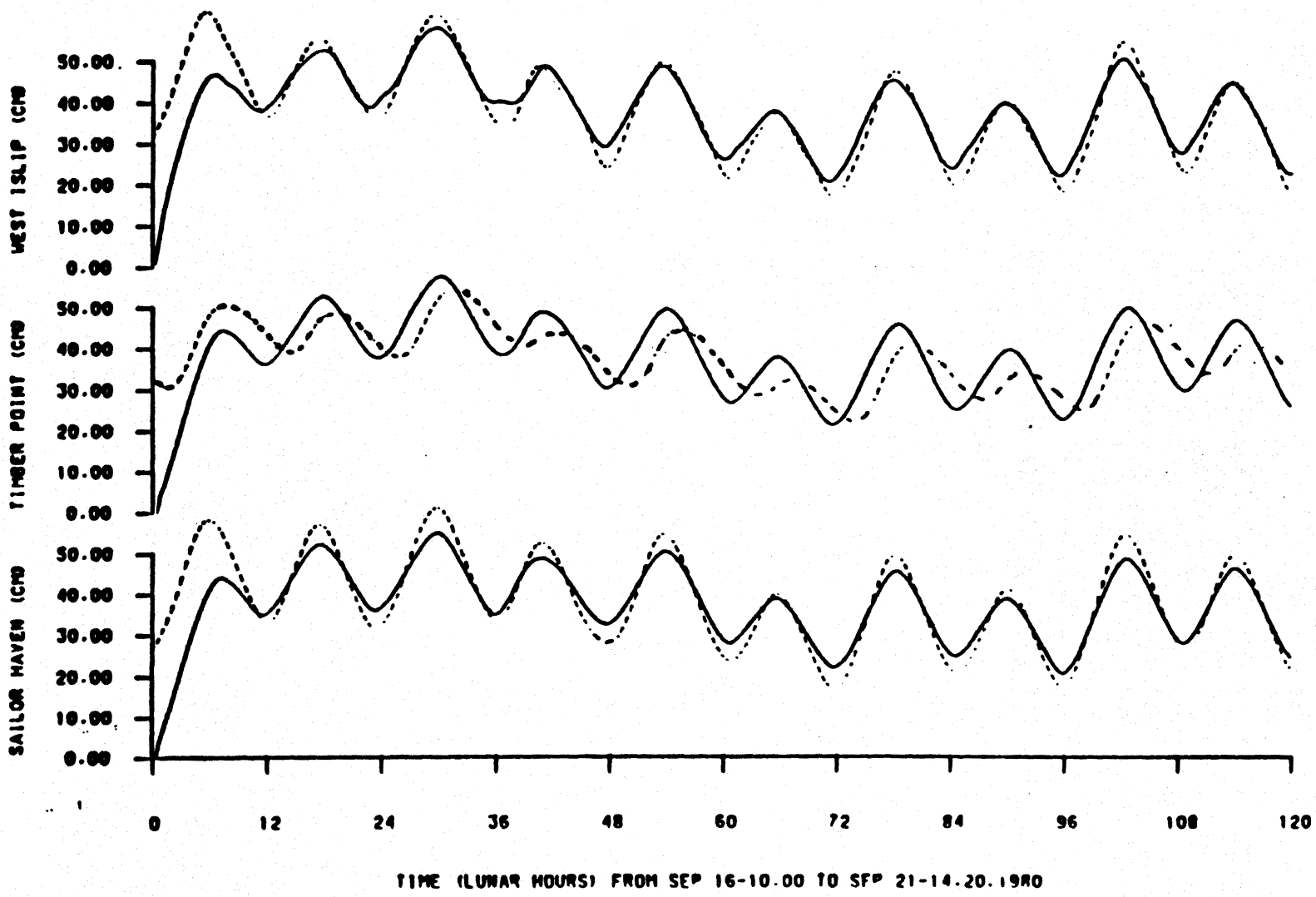


Figure 7. Observed East-West velocity component data (dashed line) and model computations (solid line) for the first calibration at Fire Island Coast Guard Station, Smith Point and Mid-Bay.

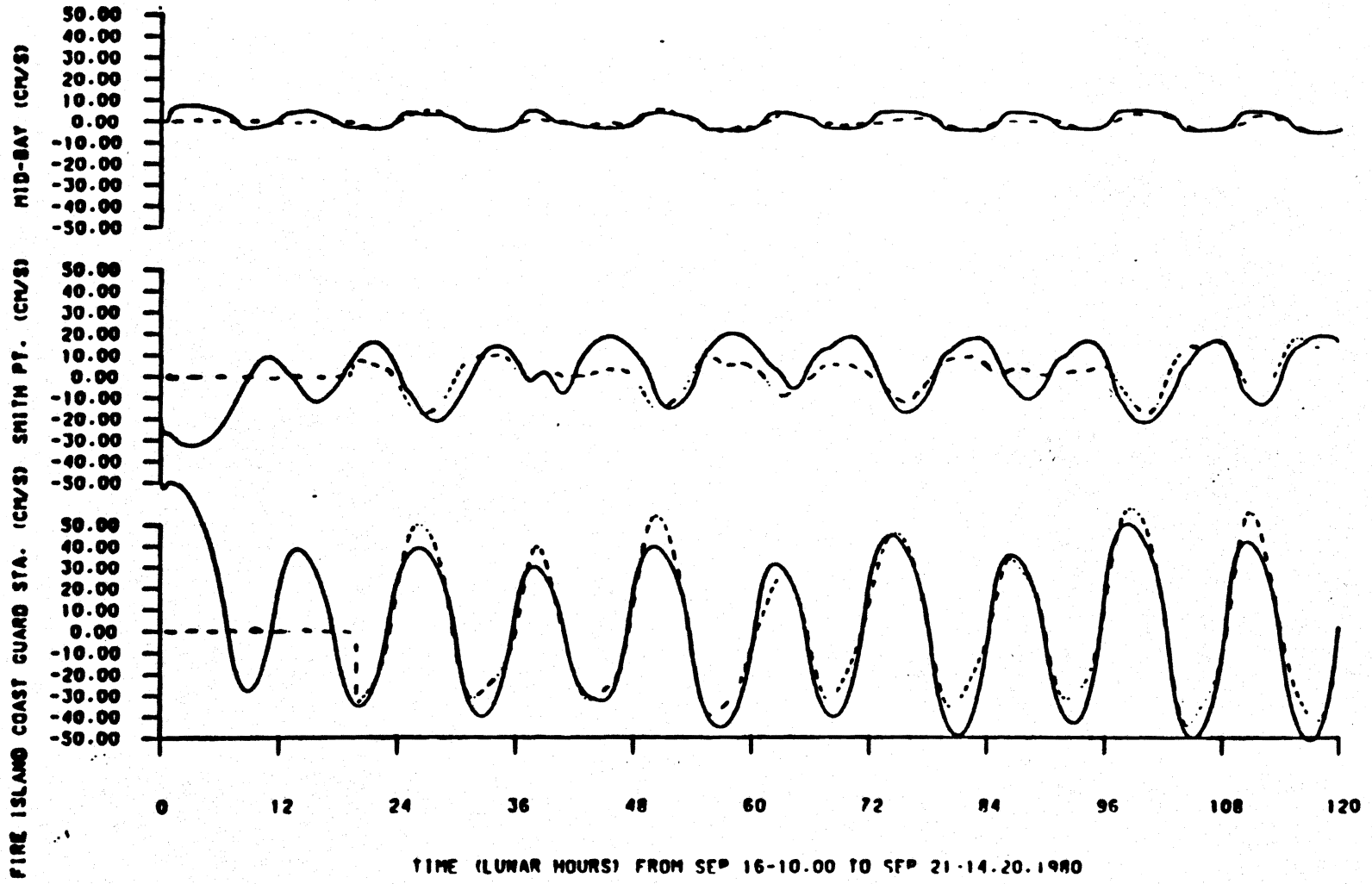


Figure 8. Observed North-South velocity component data (dashed line) and model computations (solid line) for the first calibration at Fire Island Coast Guard Station, Smith Point and Mid-Bay.

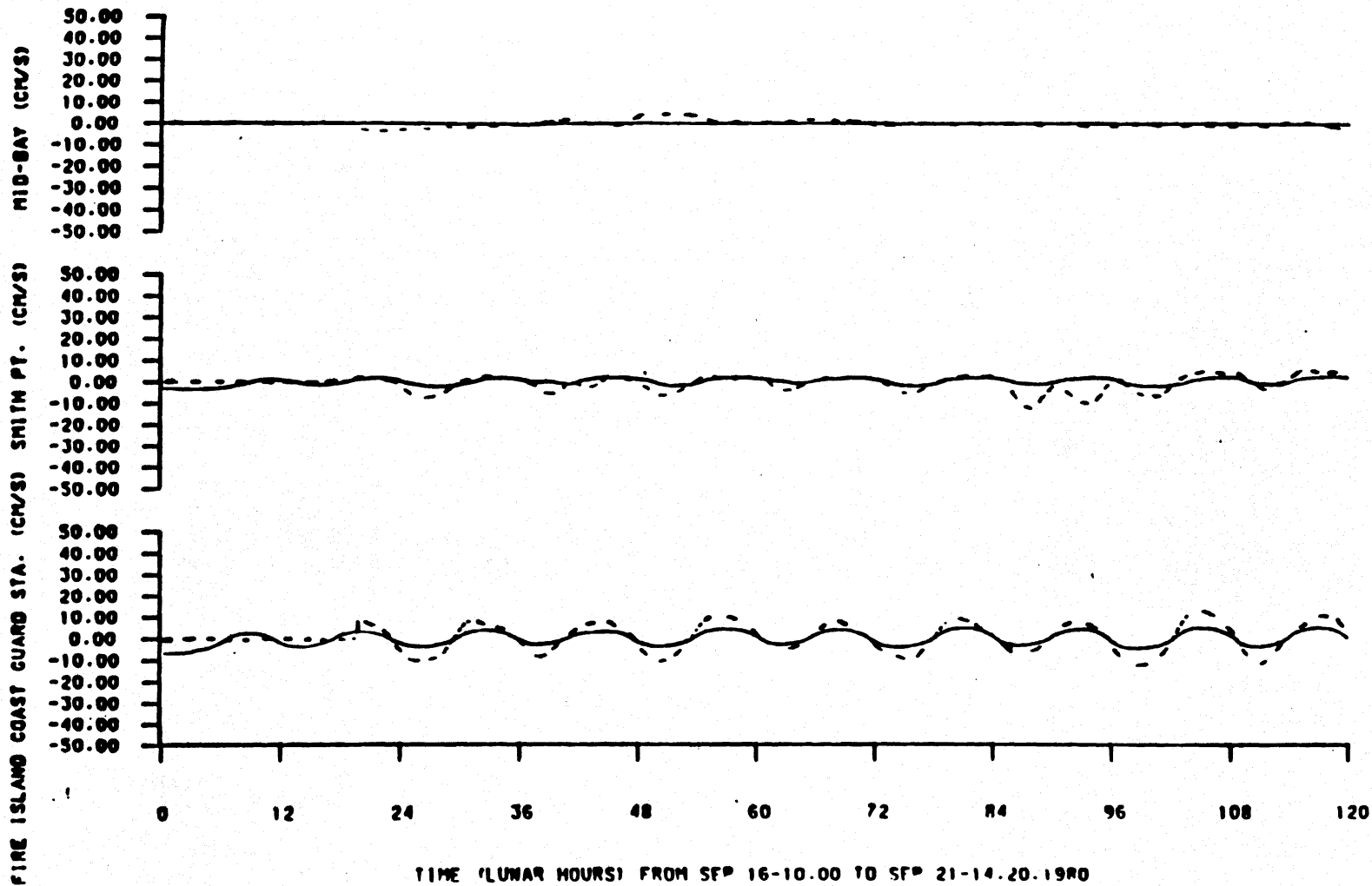


Figure 9. Observed surface elevation data (dashed line) and model computations (solid line) during the second calibration at Fire Island Coast Guard Station.

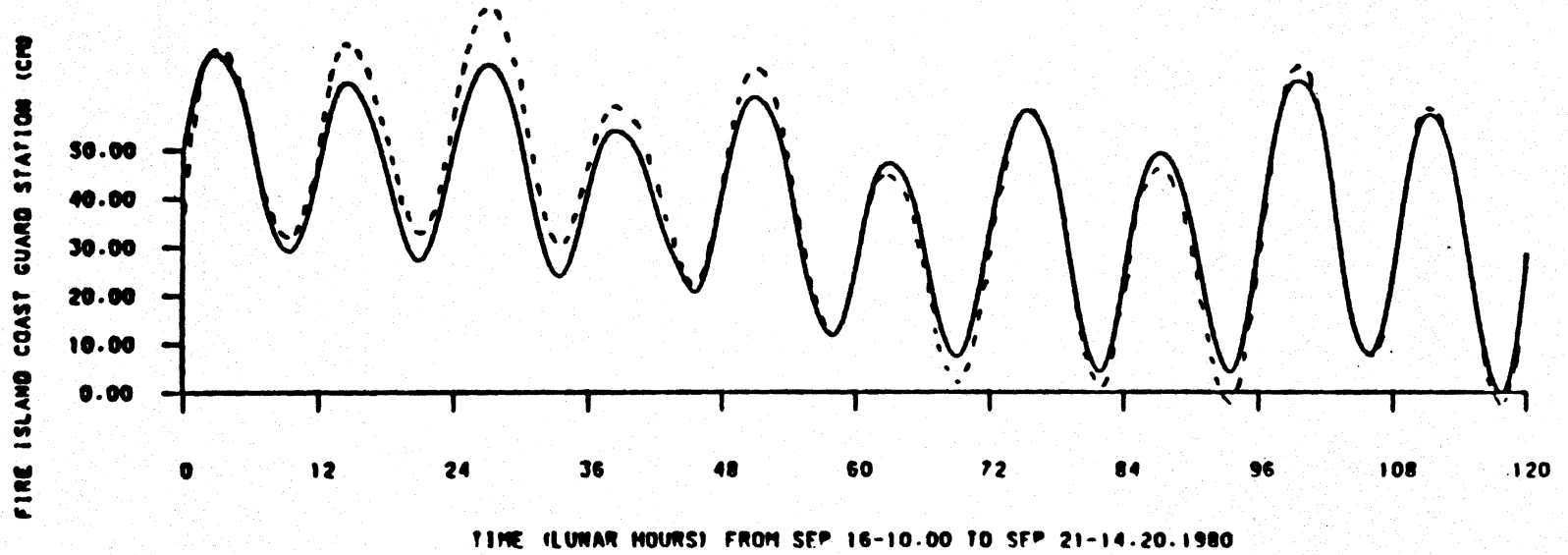


Figure 10. Spatial velocity field for maximum flood at Democrat Point, without Yellow Bar (above) and with Yellow Bar (below), for spring tide condition and medium river flow. Map scale is 1:180000. Vector scale is 1 mm = 30 cm/s.

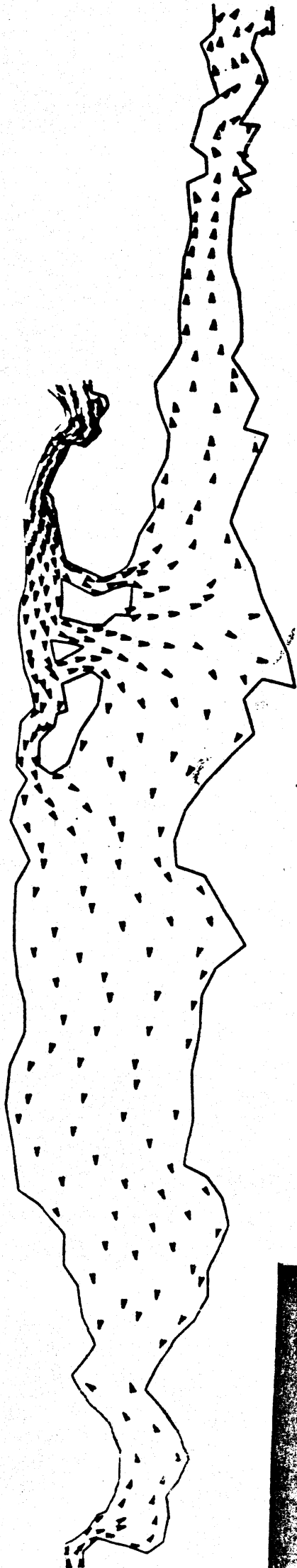
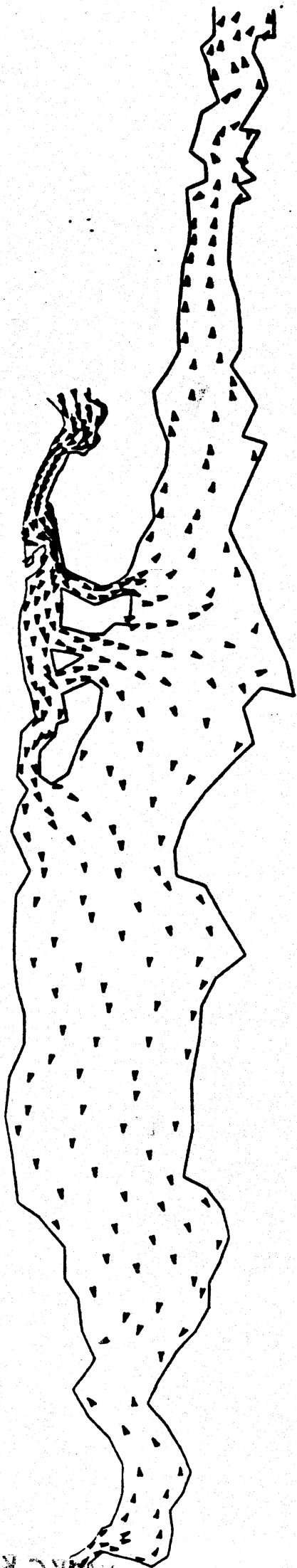
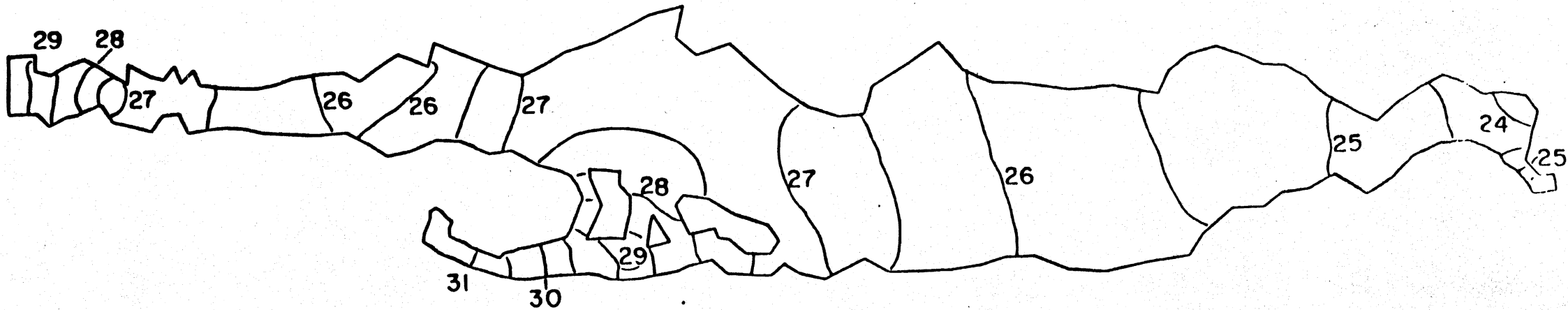


Figure 11. Spatial velocity field for maximum ebb at Democrat Point, without Yellow Bar (above) and with Yellow Bar (below), for spring tide condition and medium river flow. Map scale is 1:180000. Vector scale is 1 mm = 30 cm/s.



Figure 12. Spatial tidal mean salinity field without Yellow Bar (above) and with Yellow Bar (below), for spring tide condition and medium river flow. Map scale is 1:180000.



Page 48

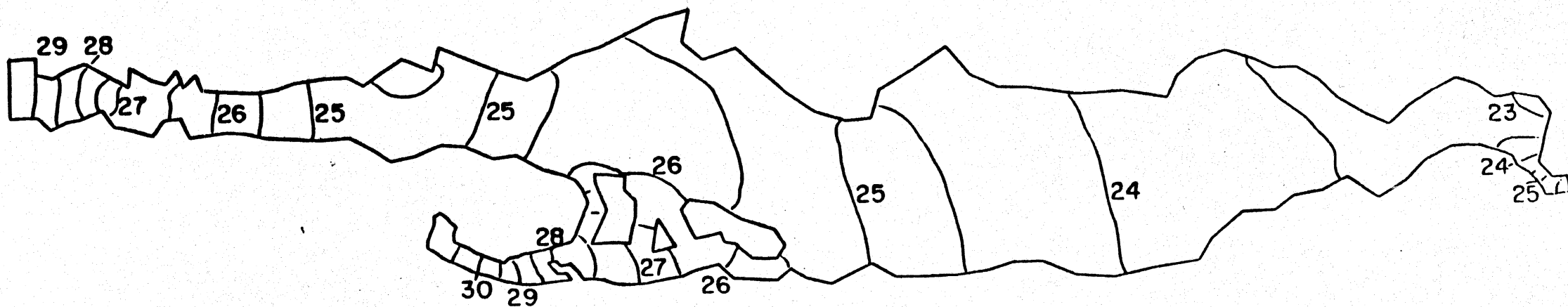


Figure 13. Spatial tidal mean salinity differences, without Yellow Bar minus with Yellow Bar, for spring tide condition and medium river flow. Map scale is 1:180000.

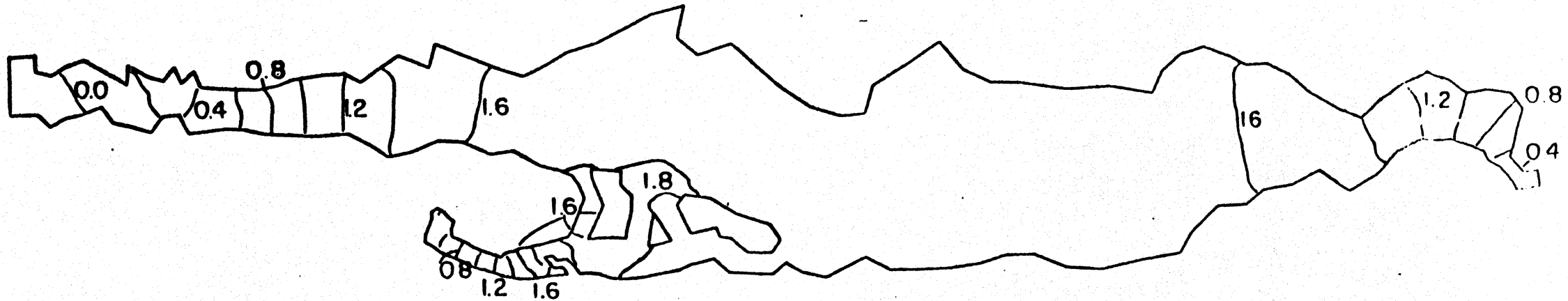


Figure 14. Spatial tidal mean salinity field without Yellow Bar (above) and with Yellow Bar (below), for spring tide condition and low river flow. Map scale is 1:180000.

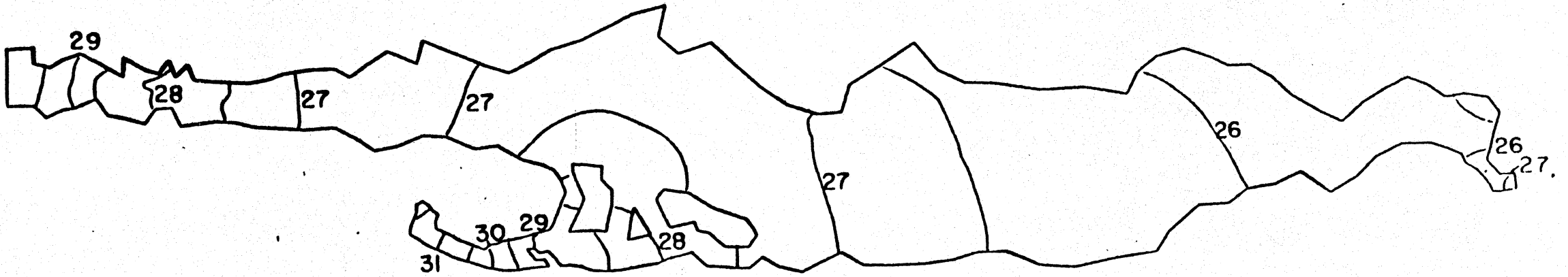
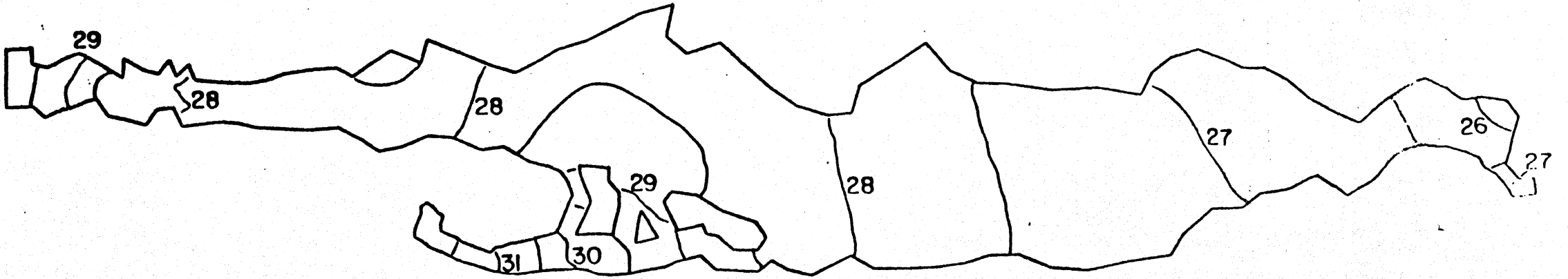


Figure 15. Spatial tidal mean salinity differences, without Yellow Bar minus with Yellow Bar, for spring tide condition and low river flow. Map scale is 1:180000.

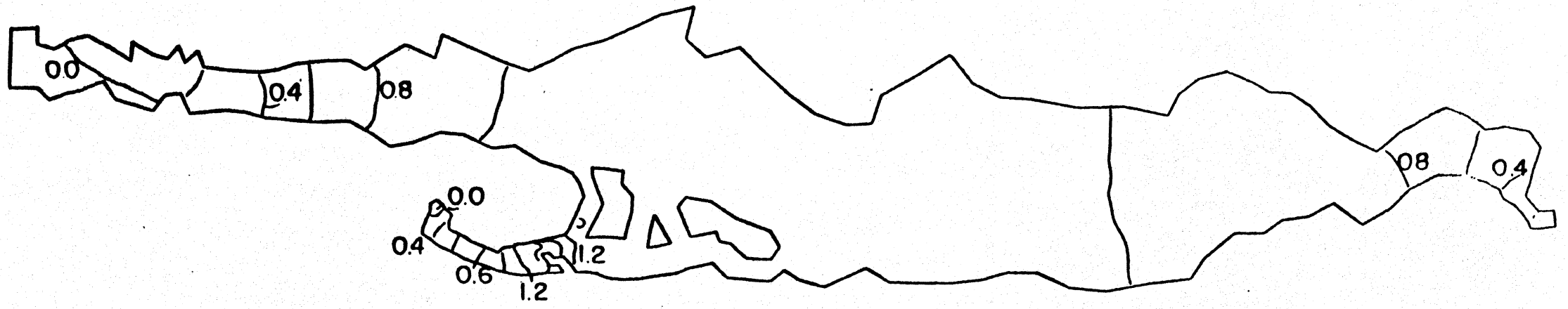
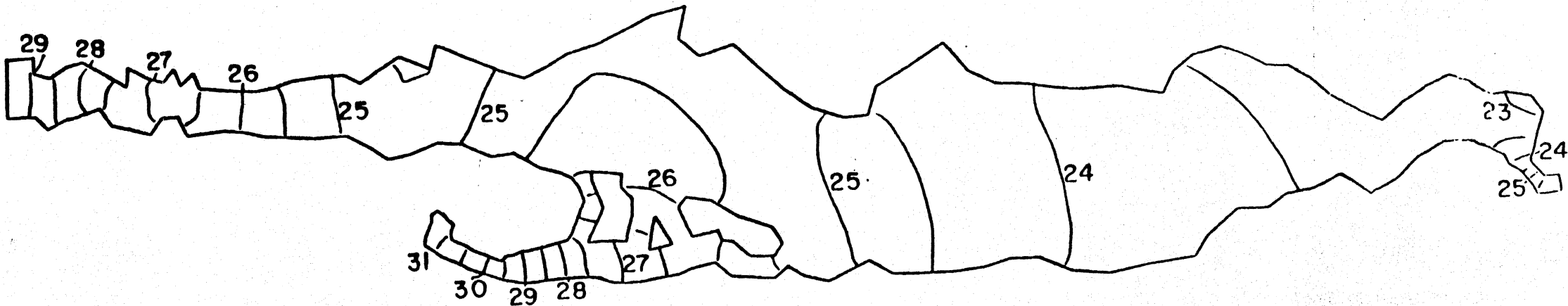


Figure 16. Spatial tidal mean salinity field without Yellow Bar (above) and with Yellow Bar (below), for neap tide condition and medium river flow. Map scale is 1:180000.



Page 56

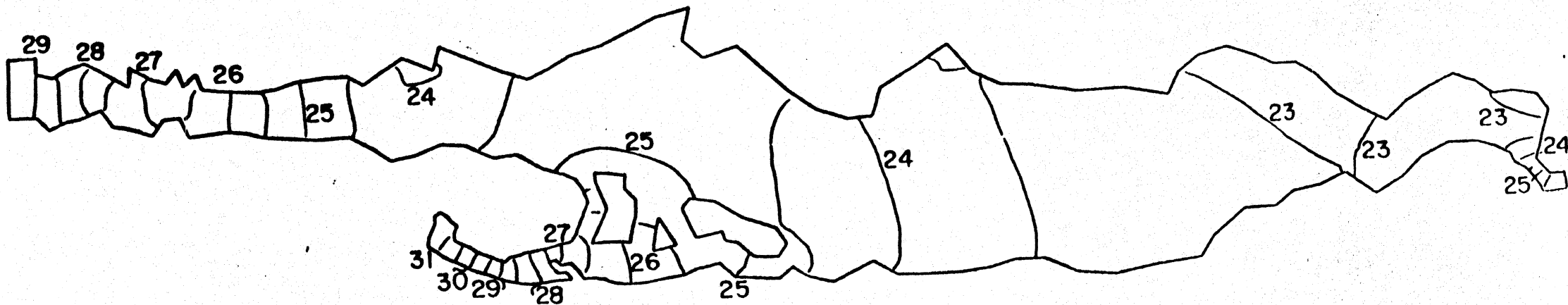


Figure 17. Spatial tidal mean salinity differences, without Yellow Bar minus with Yellow Bar, for neap tide condition and medium river flow. Map scale is 1:180000.

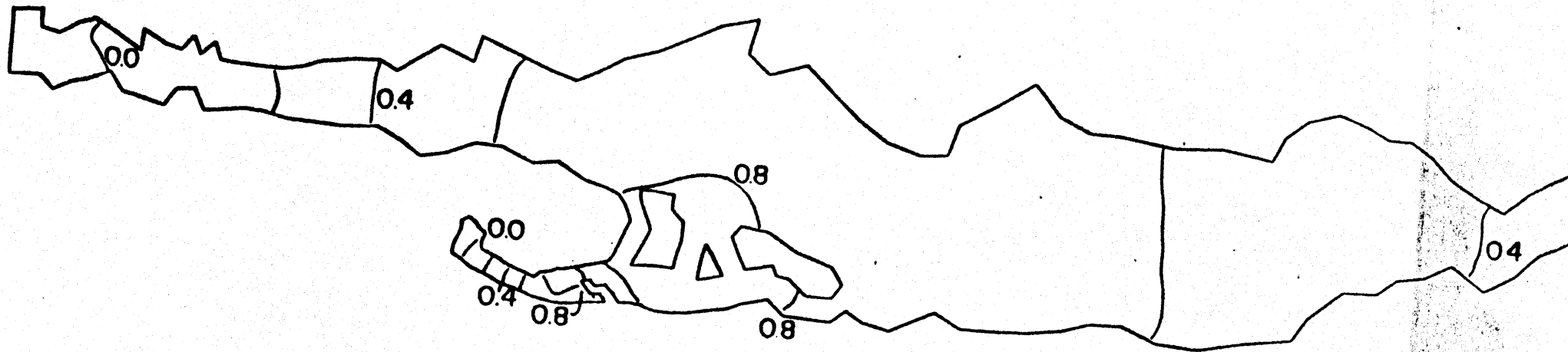


Figure 18. Spatial tidal mean salinity field without Yellow Bar (above) and with Yellow Bar (below), for neap tide condition and low river flow. Map scale is 1:180000.

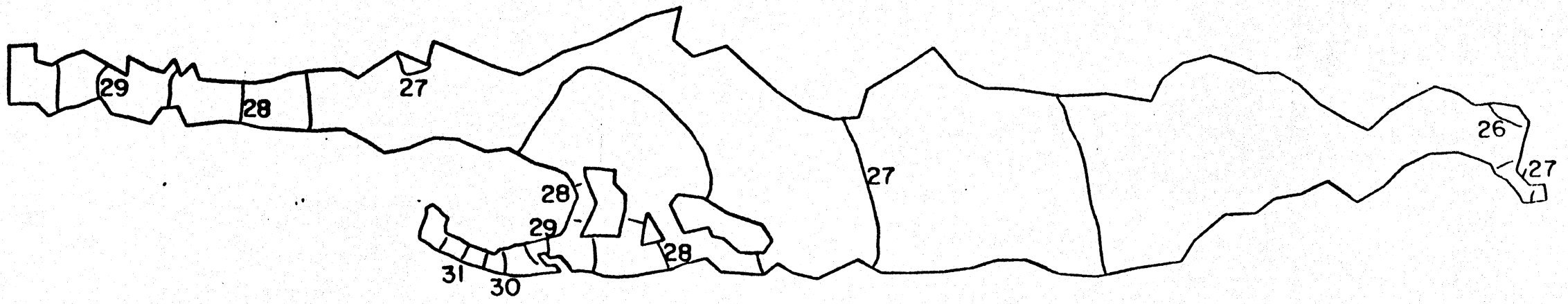
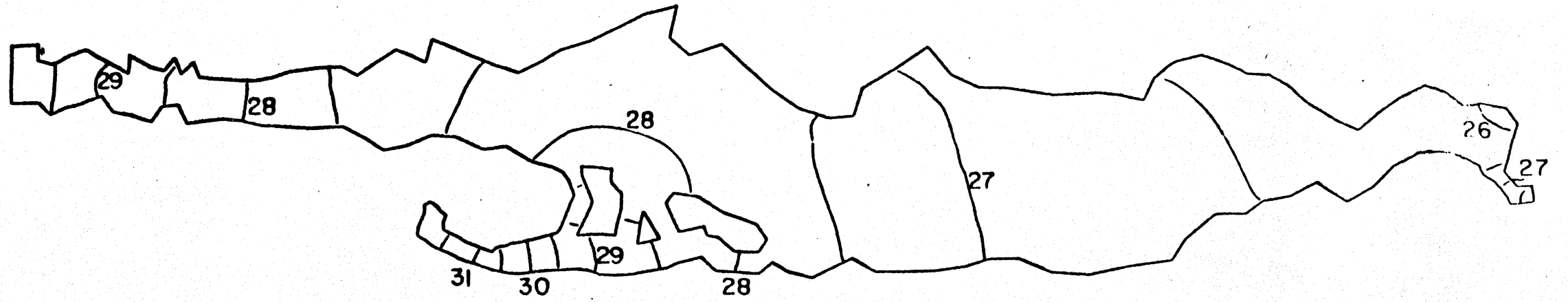
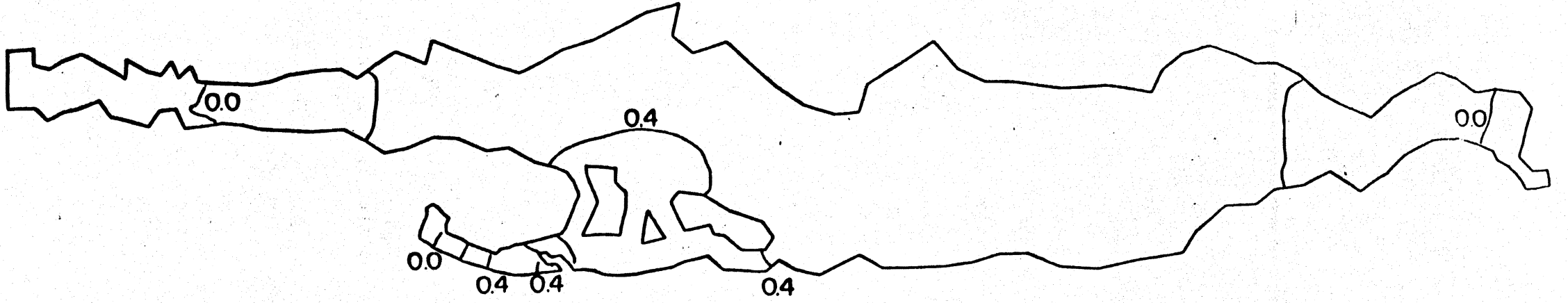


Figure 19. Spatial tidal mean salinity differences, without Yellow Bar minus with Yellow Bar, for neap tide condition and low river flow. Map scale is 1:180000.



REFERENCES

- Bokuniewicz, H.J. and M.J. Zeitlin. 1980. Characteristics of the Ground-Water Seepage into Great South Bay. Special Report 35. Marine Sciences Research Center, State University of New York at Stony Brook. 32 pp.
- Cristodoulou, G.C., J.J. Connor and B.R. Pearce. 1976. Mathematical Modeling of Dispersion in Stratified Waters. MIT, Report No. 219. Cambridge, Massachusetts. October 1976.
- Isaji, T. and M. Spaulding. 1981. Numerical Modeling of Entrainment and Far Field Thermal Dispersion for NEP I and II Power Station, Charlestown, Rhode Island. ORNL/TM-7590, January 1979.
- Kozalba, E.J. 1975. The Water Table on Long Island, New York, in March 1974. Long Island Water Resources Bull. LIWR-5, 7p, 3 pls.
- Mackenzie, C.L.Jr. 1977. Predation on Hard Clam (*Mercenaria mercenaria*) Populations. Transactions of the American Fisheries Society. 106(6): 530-537.
- McHugh, J.L. 1983. An Overview of the Hard Clam Resource. In Proc. of a Management Perspective on the Hard Clam Resource in Great South Bay, Stuart C. Buckner (ed.). Town of Islip, N.Y. March 10, 1983: 3-9.
- Pritchard, D.W. 1971. Chapter II. Hydrodynamic Models. In Estuarine Modeling: An Assessment. George H. Ward, Jr. and William H. Espey, J. (ed.). TRACOR, Inc.
- Saville, Thorndike. 1962. Factors affecting the pollution of Great South Bay, Long Island, NY, with special reference to algae blooms. Report to the Jones Beach State Parkway Authority. 31 pp.
- Suffolk County Department of Environmental Control. 1978. Interim Report on Great South Bay Salinity. May, 1978.
- U.S. Department of Commerce. 1979. Tide Tables High and Low Water Predictions 1980, East Coast of North and South America Including Greenland. NOAA, National Ocean Survey, 1979. 288 pp.
- U.S. Environmental Protection Agency. 1982. Impact Assessment on Shellfish Resources of Great South Bay, South Oyster Bay and Hempstead Bay, New York. Draft Report, Nov. 1982.
- Walka, R. 1983. Potential Effects on Changed Salinity on Clam Harvest. In: Proc. of a Management Perspective on the Hard Clam Resource in Great South Bay, Stuart C. Buckner (ed.). Town of Islip, N.Y. March 10, 1983: 15-28.
- Walters, R.A. and R.T. Cheng. 1980. Accuracy of an Estuarine Hydrodynamic Model Using Smooth Elements. Water Resources Research, Vol. 16, No. 1: 187-195, Feb. 1980.

Wang, J.D. and J.J. Connor. 1975. Mathematical Modeling of Near Coastal Circulation. MIT, Report No. MITSG 73-13. April 1975.

Wong, K-H. 1981. Subtidal Volume Exchange and the Relationship to Atmospheric Forcing in Great South Bay, New York. Ph. D. dissertation, Marine Sciences Research Center, State University of New York at Stony Brook.